Analytical Study of the Effects of Grid Resistance on Grid-Connected PV Systems: Modeling and Simulation

by

Saad Al-Gahtani

A thesis submitted to the Graduate Faculty of
Auburn University
in the partial fulfillment of the
requirements for the Degree of
Master of Science

Auburn, Alabama
May 10, 2015

Approved by

Mark Nelms, Chair, Professor of Electrical and Computer Engineering
Mark Halpin, Professor of Electrical and Computer Engineering
Robert Dean, Associated Professor of Electrical and Computer Engineering

Abstract

Lot of issues associated with grid-connected PV system have appeared. One of the issues is the variations of grid impedance. In the traditional real and reactive power calculations, the resistance of the transmission line is usually neglected. But, the resistance of the distribution line may not be negligible. In a distribution network, the R/X ratio varies between 0.5 and 7. The variations in the resistance may affect the system stability. This study presents two models of a grid-connected PV system to address the effects of the grid resistance on the system. A mathematical model is built to determine the power equations, and then, power is calculated. MATLAB is used to implement the mathematical model. Also, a Simulation model is designed and simulated in SIMPLIS to calculate the power. A set of studies is performed for both models to determine the grid resistance effects. The results from both models are plotted and compared.

Acknowledgements

First and foremost I would like to express my thanks to my parents and my wife for supporting me with love, advice and encouragement all the time since I started. I would not fulfill this without them.

I also would like to extend my thanks, appreciations and gratitude to Dr. Nelms. During my work with him, he was a friend, professor and advisor. He always inspires me and assists me to achieve my goal. It has been an honor and pleasure to work with him.

Additionally, I would like to thank my professors, Dr. Halpin, Dr. Dean, and Dr. Hung who taught me. I believe I acquired a lot of knowledge from them.

Also, I want to present my acknowledgements to my friends; Daniel and Brandon. They have been close and lovely friends since I enrolled to the program. They were collaborative and helpful with me.

Finally, I thank everyone who helped, supported, and motivated me.

Table of Contents

List of Figures

vii

List of Tables

List of Abbreviations

Symbol	Description	Unit
PV	Photovoltaic	
PWM	Pulse Width Modulation	
MPPT	Maximum Power Point Tracker	
V_1	Inverter Output Voltage	Volt (V)
V_2	The Grid Voltage	Volt (V)
I	Line Current	Ampere (A)
R	The Grid or Line Resistance	Ohm (Ω)
X	The Grid or Line inductance	Ohm (Ω)
δ	The Phase Angle of Power	Degree ($°$)
P_1	The Real Power from the Inverter	Watt (W)
Q_1	The Reactive Power from the Inverter	VAR
P_2	The Real Power of the Grid	Watt (W)
Q_2	The Reactive Power of the Grid	VAR
THD	Total Harmonic Distortion	
V_c	The Voltage of the Control Signal	Volt (V)
V_t	The Voltage of the Carrier Signal	Volt (V)
f_s	The Frequency of the Control Signal	Hertz (Hz)
f_t	The Frequency of the Carrier Signal (Switching Frequency)	Hertz (Hz)
f_c	Cut-off Frequency	Hertz (Hz)
m_a	Modulation Index	
m_f	Frequency Index	
L_f	Filter Inductance	Henry (H)
C_f	Filter Capacitance	Farad (F)

1. Introduction

This research presents a study and analysis of the effects of the line impedance, or grid impedance, on the maximum power transfer from photovoltaic (PV) panels to the grid through an inverter. The study concentrates on the effects of the resistance of the grid impedance. In most studies, the resistance of the line is neglected, or the R/X ratio is equal to zero. But, this study takes the resistance of the line into account and investigates the effects of including it in the models presented in the study. A mathematical model is examined in MATLAB. Also, a grid-connected inverter is modeled in SIMPLIS to examine the effects of the resistance on the system. Finally, the results of both models are compared. This research is introduced by three main concepts: Renewable Energy, Solar Energy, and PV Systems.

1.1 Renewable Energy

One of the world's biggest issues in this century is the need for sufficient energy that fits with the increase of global population. The global population increases yearly and the demand for energy resources increases.

The energy used every day is mostly from conventional sources, which depend on petroleum and oil products. But, oil is not a permanent resource and it is estimated to be depleted in the near future. Also, the conventional sources cause environmental issues, one of which is CO_2 emissions [1]. Searching for new resources of energy is necessary to have an unlimited supply of energy for the future. This involves finding renewable energy sources that are available wherever they are needed, being able to convert the energy from one form to another form and then use it without creating any

1

problems, such as pollution, are among some of the most significant requirements that our world needs addressed [2].

Economic growth is highly based on the conventional sources operated by oil, natural gas, and coal [3]. But, the continuous reduction of the conventional sources means that some type of energy source is needed to meet the rising energy demand of the world [1-3]. Because of the environmental issues caused by the conventional sources, looking for efficient and environmentally-friendly energy is becoming essential [3]. The concern of protecting the environment and searching for green energy points to the use for renewable energy.

The renewable or sustainable energy is the energy that can be continuously reproduced from nature; thus, the renewable energy sources produce unlimited energy. Renewable energy comes from the sun directly (e.g. thermal) or indirectly (e.g. wind and biomass) and can be derived from the movement of the particles in the environment such as moving water. Renewable energy is then converted to a different form of energy. Different sources of renewable energy are shown Fig. 1.1. Also, the market for renewables is increasing as people accept using these new energy types. [3]
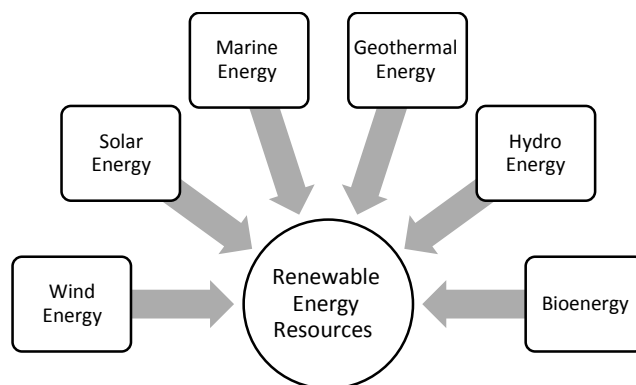
Fig. 1.1: Renewable energy resources [3].

From Fig.1, there are six main resources for renewable energy. Each one has its characteristics and properties. In order to understand the mechanism of each energy type, the energy types have to be known. The energy is classified into two main types: kinetic energy and potential energy [4]. Kinetic energy can be found in the moving particles (such as wind), while potential energy presents in the position between those particles (such as stored water in dams and gasoline). These two main types of energy can be converted to other forms of energy such as mechanical, electrical energy, thermal energy.

The renewable energy resources are described as following [3]:

1. Wind Energy:

   The wind energy is converted to other forms of energy such as electrical energy.

2. Solar Energy:

   The solar energy is converted to electricity by PV cells or into a thermal energy.

3. Marine Energy:

   The marine energy is the energy from oceans and it comes in different forms such as waves, tidal currents, and ocean currents. This energy can be converted to a usable form.

4. Geothermal Energy:

   It is the energy from the earth.

5. Hydro Energy:

   Hydropower is the power produced from the energy of moving water and flowing water; it can be converted to electrical energy.

6. Bioenergy:

Bioenergy or biomass, from organic material, is the converting of biomass into another form of energy.

The amount of each energy in nature is given in Fig. 1.2.
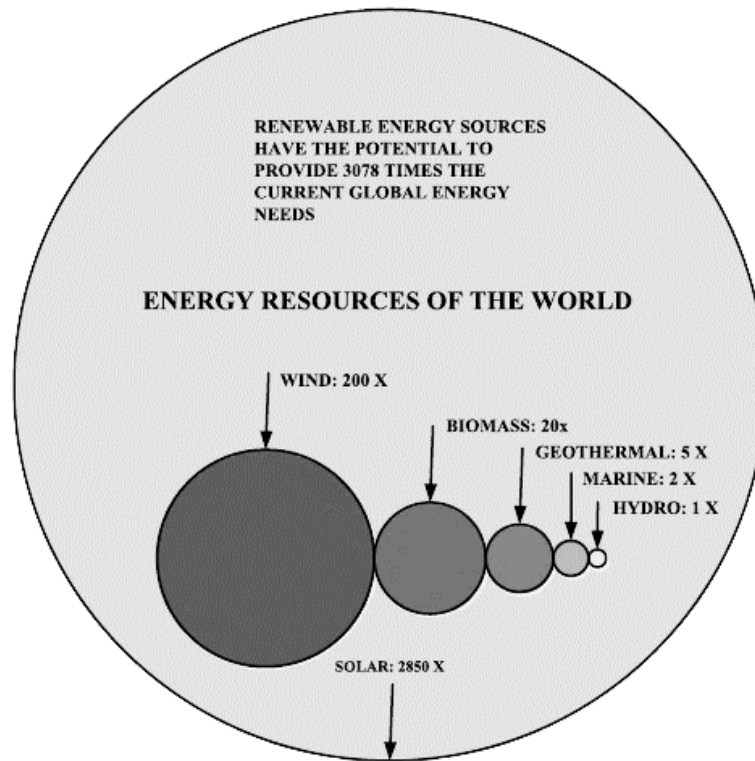
Fig. 1.2: Energy resources in nature [3].

1.1.1 Advantages and Disadvantages of Renewable Energy

Advantages of using renewable energy are as follows:

1. The renewable energy resources are inexhaustible and provide an unlimited supply of energy.

2. The energy is clean.

3. It helps in reducing CO_2 emissions.

4. It can be stored in batteries when it is not usable.

Disadvantages include the following:

4

1. It is not reliable.

2. Biomass causes air pollution.

3. The installation and maintenance are costly.

4. Some sources may not be cost effective.

These are the general advantages and disadvantages of renewable energy resources. [1][2]

1.2 Solar Energy

The sun is a very huge plasmatic ball consisting of hydrogen (92%), helium (8%), and some other elements. It is plasmatic because the nuclei and the electrons are separated due to the high temperature: 6000 K. For that, the kinetic energy between the electrons and the nuclei is very large. The power the sun sends into space is about $3.8*10^{26}$ W. Our planet receives only $1.73*10^{17}$ W, a very small amount of the sun's emitted energy, at the top of the atmosphere. [4]

The amount of the power the earth receives from the sun is equal to the power produced from about a hundred million modern power stations based on fossil fuel and nuclear power. Most of that energy goes to the oceans while some energy is interrupted by clouds and dust in the air. The energy from the sun can be categorized into two types: direct energy (e.g. solar energy) and indirect energy (e.g. wind, biomass, marine, and hydropower). The power density of the sun above the atmosphere of the Earth is known as the solar constant, and it is estimated to be 1366 W/m^2. The amount is decreased by 30% due to the atmosphere providing an insolation at the Earth's surface of about 1000 W/m^2 on a clear day at sea level. Moreover, the average power density that the Earth receives yearly, annual mean insolation, is an important quantity. It can be calculated by dividing the solar constant

by 4. This quantity is averaged over day and night, summer and winter, and differs from year to year. An important characteristic that has to be taken into account is the range and the intensity of the wavelengths of the emitted radiation. This is essential because the response of different solar cells to various wavelengths is diverse. Additionally, the solar cells installed near or at the ground collect the solar radiation directly and indirectly. The indirect radiation can be classified into two components:

1. The diffuse component: the radiation scattered by clouds and reflected by the dust in the atmosphere.
2. The albedo component: the radiation reflected from the ground or the objects such as buildings.

The direct, diffuse, and albedo components are the main factors that drive the electrical output from the solar cell [5].

1.3 Photovoltaics (PV)

PV is used in converting solar energy into electricity [3][4]. PV has a photoelectric characteristic. Radiation is absorbed, then an electron is fed and gains kinetic energy which transfers the electron to another level of energy. Also, PV is made from a thin layer of semiconductor material. Semiconductors are the principal material of PV cells, which are used in many applications such as calculators, cars, space, and so on.

PV cells can be systemized into three main systems [5]:

1. Stand-alone PV system:

   Example from its applications:

   - Solar boats
   - Calculator.

6

- Solar cars

- Water pumping

2. Grid-connected PV system:

   Example from its applications:

   - Some utility companies in the U.S. are turning to large PV systems in order to meet peak power demand and avoid building new power plants.

   - PV panels installed on the roofs and connected to the grid.

3. Hybrid System:

   Example from its applications:

   - PV-wind-diesel system

   - PV-diesel system

1.3.1 PV Physics

The structure of the electron, especially the external electron structure of the molecules or atoms, illuminates nearly all the properties of materials: mechanical, electrical, chemical, thermal, and biological. The measurement unit of the charge (Q or q) is coulombs (C). An electron has a charge of $1.6*10^{-19}$ C, positive or negative. The charged particles generate electrical fields (E). E is a vector meaning that it has a magnitude and a direction. The charged particles located in an external E are moved due to the force from E. Then, the movement of the particles produces energy as well as an electrical potential. The current is created from the flowing of charges. The electrical characteristics of the materials are classified into three general types: conductors, semiconductors, and insulator. Because semiconductor is the primary material of a PV cell, it will be discussed in the next section.

1.3.2 Semiconductors of PV

The most common used semiconductor is silicon and has been used extensively by PV cell manufacturers for many years [5]. The silicon solar cell can be categorized into three types [5, 6]:

1. Monocrystalline:

   This type has the highest efficiency among the types of silicon solar cell. The shape of its cell is hexagonal, so a module can take more cells. The efficiency of the module ranges from 12-16%. Notice that a cell efficiency is higher than that of a module because of the empty spaces between cells in the module. Also, the module surface area of about 7 m^2 provides 1 kW.

2. Multicrystalline:

   It is made from pure silicon using a molding process. The shape of its cells is square or rectangular. The efficiency varies from 11-15%. The module surface area of about 8 m^2 produces 1 kW.

3. Amorphous:

   Most people have seen this type in many applications such as calculators and solar light. Amorphous is the cheapest type and has the lowest efficiency of 6-8%. The required module surface area to produce 1 kW is about 16 m^2.

1.3.3 Advantages and Disadvantages of PV

According to [4],

The advantages of PV are:

1. Reliable systems.

2. The operating point is low.

3. Modularity.

, and the disadvantages are:

1. The installation is costly.

2. Unpredictability.

3. The storage is costly.

4. The infrastructure in remote areas is lacking.

2. Grid-Connected Inverter

The inverter is the main component of a grid-connected system, because it converts DC voltage into AC voltage. The inverter has the ability to produce AC voltage that has the same frequency and amplitude as the grid using advanced electronic elements. [5]

2.1 Inverter Topologies

The inverter has to execute three functions to supply the energy to the grid. These functions are as following:

1. Shaping the current into sinusoidal waveform.

2. Inverting the DC current to AC current.

These functions help in determining the required components to build the inverters and shaping them. The price of an inverter can be determined by these functions performances. [7]

There are four main topologies of solar power inverters:

1. **Central Inverters:**

The first PV inverters were line commutated with rated power of several kilowatts. A central inverter is shown in Fig. 2.1. The advantages of this topology include robustness, high efficiency and cheap cost, but the big deficiency is a low power factor which ranges between 0.6 and 0.7. The power factor can be improved by adding filters, which can decrease the total harmonic distortion. [7]
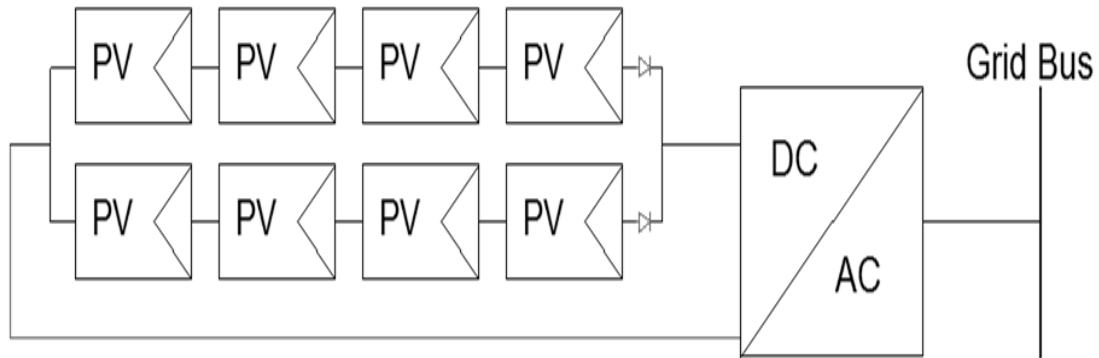
Fig. 2.1: A central inverter.

Another topology came after the developments of semiconductor technologies. Thyristors were used in the old inverters, but in the modern inverters, they are replaced by BJT's, MOSFET's and IGBT's. These semiconductor devices are switching devices and have high frequency switching rates above 16 kHz. Currently, most central inverters available in the market are of self-commutated type. The power rating of this topology is above 2 kW. They can be designed with and without transformer(s). They are combined with a PWM full bridge switching at high frequencies. The switching frequencies are responsible for shaping the current. The bridge is composed of IGBT's or a combination of MOSFET's and IGBT's. These inverters are robust, efficient and cheap, but the drawback is that the efficiency is lower than that of line-commutated topology because of high switching frequency. Additionally, an inverter topology having several transformers is known as a magnetically coupled inverter. This topology is composed of several transformers connected to the midpoints of several conventional single-phase full bridges from the primary windings, and the secondary windings of those transformers are connected in series. The inverter is able to produce 3^n, where n is the number of transformers, combinations generated from different nodes of voltage at the secondary windings.

11

The benefits of this inverter topology are low switching frequencies which makes shaping an accurate sine wave simple, robust, and cheap. The main disadvantage of this inverter topology is the presence of several transformers. [7]

2. Module Integrated Inverters(Module Oriented Inverters):

Module integrated inverters can be modeled with one or several PV modules [7]. This makes each module an equivalent AC power source as shown in Fig. 2.2 [5]. The power rating of this topology is below 500 W and the output voltage of PV array is between 30 and 150 V. Because of the low voltage levels, a voltage adjustment element is added to the system. Also, different topologies can be designed due to low voltage levels [7].
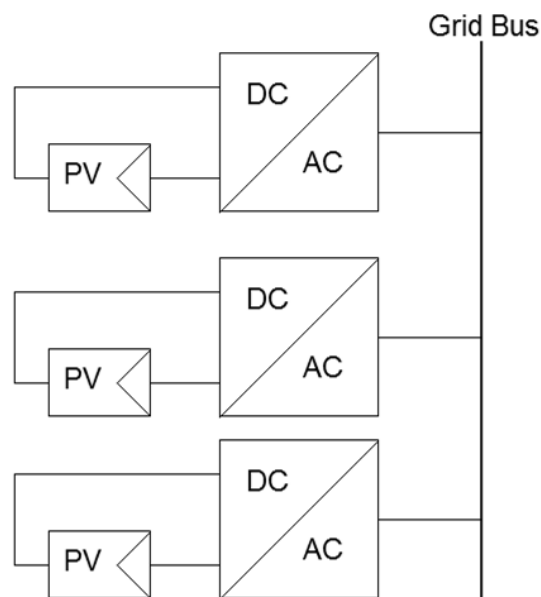
Fig. 2.2: Module integrated inverters.

A topology of Module integrated inverters has a line frequency transformer which allows use of low voltage MOSFET's for a PWM high frequency switching bridge. Moreover, this topology is fitting for the high current produced by PV modules. The control system is set at the low voltage side. MOSFET's are used in large quantities

because of their low prices. An inverter of a line frequency transformer provides some advantages including reduced magnetic components and cost. [7]

Once again, a variety of topologies can be modeled due to low voltage levels of PV modules. Some topologies do not have a transformer in order to decrease the number of magnetic components and increase the efficiency. A boost converter can be used to boost PV module voltage. The output current is shaped and inverted by the second converter stage at the high level side. [7]

The advantages and disadvantages of using module integrated inverters are listed below [7].

Advantages:

  a. The system is at the highest level of flexibility.

  b. Each PV module has its own MPPT.

  c. DC wiring is not required.

  d. The system is cost-effective.

Disadvantages:

  a. These inverters are expensive.

  b. If an inverter fault occurs, it is difficult and has a high cost to replace that inverter.

  c. The system cost might also be increased in order to have specific safety requirements.

  3. **String Inverters:**

String inverters are able to have the advantages of both central inverter and module integrated inverter. The PV array consists of several PV modules connected in series

as shown in Fig. 2.3. The power range of these inverters is up to 2 kW; at this power

range, the voltage levels range between 150 V and 450 V. A number of topologies can

be applied based on these power and voltage ranges. IGBTs and MOSFETs are used

with switching frequencies of 16 to 32 kHz. The advantages of string inverters include

the following:

    a. These inverters can be used at high power.

    b. The efficiency is increased by 1-3% compared to central inverter.

    c. The cost per watt is decreased. [7]
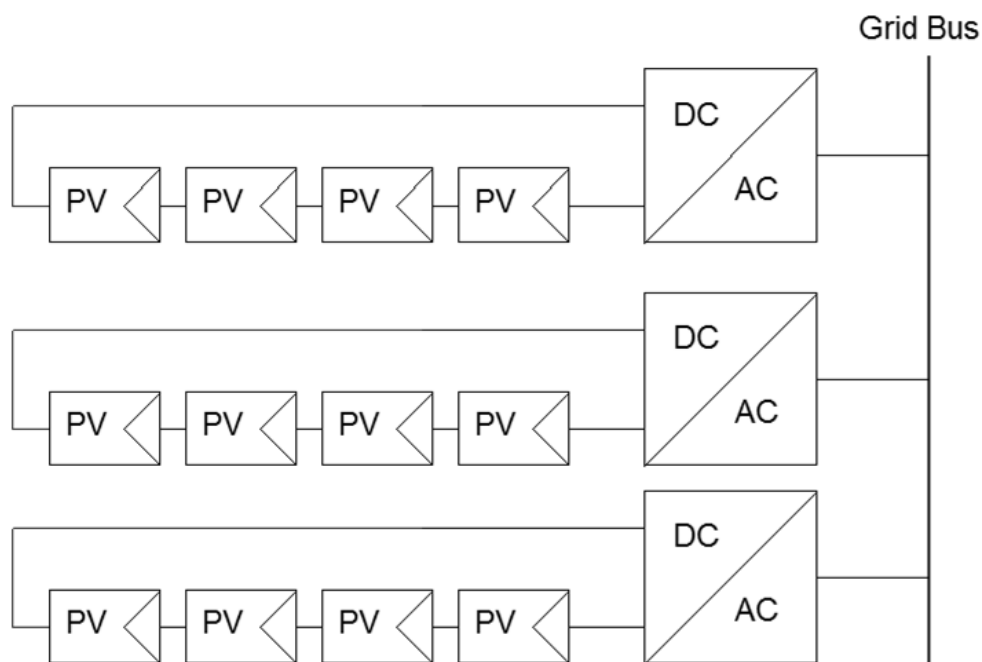
Fig. 2.3: String inverters.

4. Multi-String Inverters:

The goal behind designing this topology of inverters is to lower the cost of inverters

by 20%. Fig. 2.4 shows the configuration of a multi-string inverter. These inverters

can combine the advantages of the low costs of the central inverters and of high

energy output of a string inverter. A topology consists of lower DC-DC converters connected to single PV strings where each PV string has its own MPPT to optimize the power output and a DC bus connecting all converters through a central inverter according to the size of PV string. IGBTs are used in the central inverter, thus it is a PWM inverter. The system can be expanded by adding more PV strings. Each PV string is connected to a DC-DC converter. The voltage varies between 125 and 750 V, the power ranges up to 5 kW. [7]
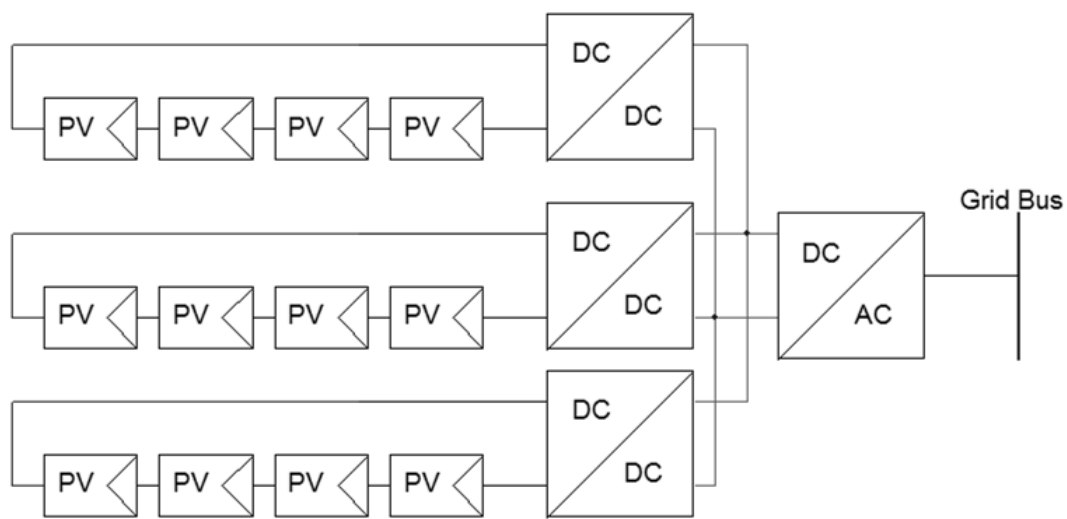
Fig. 2.4: A multi-string inverter.

Moreover, multi-string inverters have a unique feature that makes them fit to use in reactive power compensation, and these inverters can produce high voltage and high power. Another feature is that as the voltage levels increase, the harmonic content remains low without transformers or switching devices. That is because the structure of multi-string inverters looks like multilevel voltage sources. There are three common topologies of multi-string inverters: diode clamped multilevel inverter, flying capacitor multilevel inverter, and Cascade multilevel inverter [8].

The line-commutated and transformerless inverters topologies achieve the maximum efficiency rate of about 96%. The improvement of switching devices and higher DC input voltage results in improving the efficiency. [7]

2.2 New Trends in Inverter Topologies

The major drawback of the single inverter is that it needs large electrolytic capacitors at the input of the inverter. These capacitors impact the efficiency, cost and lifetime of the inverter. As a result, small three-phase inverters have been developed to decrease the size of the electrolytic capacitors. [7]

Additionally, the string technology is combined with master-slave concept in large PV plants. Parallel PV strings are connected to an inverter at low solar irradiation. As irradiation increases, PV strings are separated from each other and each is connected to an inverter. This combination allows the efficiency to increase by 2% [7].

2.3 Issues with Grid-connected Inverter

The choice of inverter depends on several factors such as output power rating, maximum power point tracking (MPPT) rating, shading and weather conditions. Inverters have to deal with the power coming from PV panels under a wide range of conditions that affect the characteristics of the power system. They can handle these conditions by using MPPT, which are used to control and optimize the energy supply. The efficiency is the most significant characteristic by which an inverter is selected in a certain application. The DC to AC converting efficiency can reach up to 98%. But, the efficiency drops if the inverter operates below about 25% of its maximum power rating. Shading issues can be solved by using string inverters. For example, if the power system with a central inverter suffers from a shading problem, the central inverter can be replaced by a number of string inverters. For those inverters having

the transformers, the efficiency is reduced slightly due to the heat produced by transformers. Therefore, inverters must have a cooling system in order to be highly efficient. Also, the cooling system becomes more important as the inverter power capacity increases. Because the inverters are connected to the grid, the islanding issue is very dangerous. For that, the inverters have to be disconnected when the grid is shuts down due to a fault or maintenance to avoid having voltage on the grid, especially the grids of large systems. The power factor and the waveform of the inverter must be compatible and agreeable with the grid output. Sensitivity to voltage, frequency and impedance fluctuations are important features that the inverter must have in order to be connected to the grid. These features allow the inverter to shut down if these terms deviate from their set points. The technical performance of the inverters is examined based on several aspects as following:

1. Lighting and surge protection.
2. Safety.
3. System reliability.
4. Inverter sequencing.
5. The connection mode of PV modules into strings or arrays. [5]

2.4 The Effects of the Line Impedance on the Grid-tied PV System

The line impedance is usually represented as an X/R ratio in power systems. The variations in the X/R ratio have noticeable impacts on the grid-connected PV systems [9]. The transmission line is usually inductive in the high-voltage grid while in the low-voltage grid the transmission line is mostly resistive [10]. The reason that the line resistance is considered is that the line or the feeder does not have an inductor or a transformer [10]. Therefore, the X/R ratio is very small. In other words, R/X ratio is

17

very high in a low-voltage network. The R/X ratio on high-voltage lines are usually under 0.5, but in the low-voltage line it varies between 0.5 and 7 [11].

In a typical system, the phase angle is related to active power and the voltage difference is related to reactive power [12]. The X/R ratio is decreased as the system operates and that means the resistance value is increased [12]. The variations in line impedance affect the steady-state conditions of the power system. Small variations do not affect the stability of the system [13]. But, large variations in X/R ratio, because of increasing R, impact the system, and make it unstable [12].

3. Grid-connected PV System Modeling

The design of grid-connected PV system mainly depends on the design and specifications of the inverter. The grid-connected inverters come in many forms. The selection and the design of an inverter are dependent on the inverter application where it is installed. Also, other specifications such as grid codes and regulations have to be met in order to operate the inverter [14]. The inverter modeled in this research is a single-phase inverter. The topology being used is a simple full bridge single phase configuration. The configuration chosen is simple and well documented. Also, it is a basic topology to add additional components to the inverter.

3.1 Mathematical Model of the Grid-connected PV System

The goal of creating a mathematical model of the grid-connected PV is to find the power equations of the system. The power equations are calculated using power flow methods. The following features are desirable in any grid-connected inverters: output power regulation, high power quality, high efficiency, high reliability, low cost, low total harmonic distortion (THD), high robustness to perturbations, fast dynamic response, and simple circuitry [15-17]. The inverter also requires information about the phase angle, amplitude, and the frequency of the grid voltage [18]. Power flow analysis of the system helps in providing the grid information and in designing a control system to achieve the above features [15] [18]. A mathematical model of the grid-connected inverter is created to calculate the power flow of the interested grid-connected PV. Per-unit is used in the calculations of the mathematical model. MATLAB is used to implement the power equations.

3.1.1 Derivation of Power Flow Equations

Fig. 3.1 shows a simple representation of the inverter output and the grid. The two active sources shown in the figure represent the inverter output ($V_1 ∟δ$) and the grid voltage (V_2). Power transfers from source 1 to source 2. The power at source 2 is calculated using three different methods.
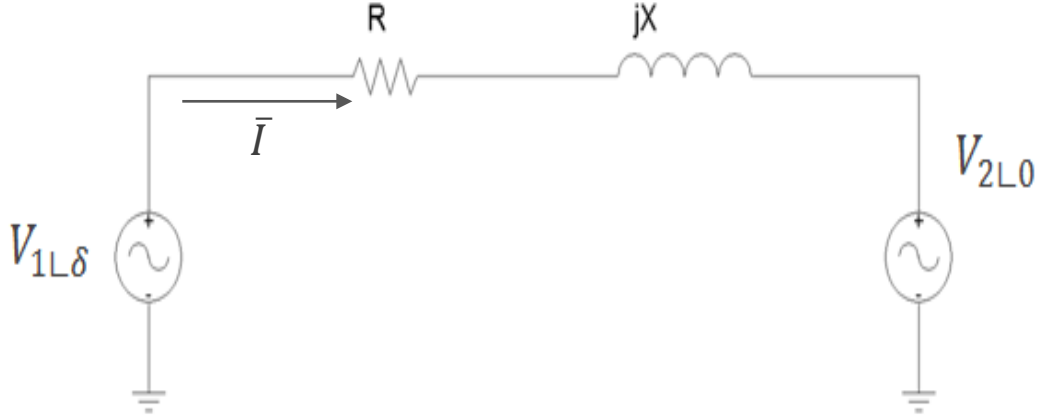
Fig. 3.1: Grid-connected inverter model from the grid side.

$$\bar{S}_1 = P_1 + jQ_1 = \bar{V}_1 \bar{I}^* \qquad (3.1)$$

$$\bar{I} = \frac{\bar{V}_1 - \bar{V}_2}{R + jX} \qquad (3.2)$$

$$\bar{S}_1 = \left(\frac{R\bar{V}_1 - R\bar{V}_2 - jX\bar{V}_1 + jX\bar{V}_2}{R^2 + X^2} \right)^* \bar{v}_1$$

$$\bar{S}_1 = \frac{\left(\begin{array}{c} RV_1{}^2\cos^2\delta + RV_1{}^2\sin^2\delta + jXV_1{}^2\sin^2\delta + jXV_1{}^2\cos^2\delta - RV_1V_2\cos\delta + XV_1{}^2\cos\delta\sin\delta \\ -XV_1{}^2\cos\delta\sin\delta + XV_1V_2\sin\delta - jXV_1V_2\cos\delta + jRV_1V_2\sin\delta - jRV_1{}^2\sin\delta\cos\delta + jRV_1{}^2\sin\delta\cos\delta \end{array} \right)}{R^2 + X^2}$$

$$P_1 = \frac{RV_1{}^2 - RV_1V_2\cos\delta + XV_1V_2\sin\delta}{R^2 + X^2} \qquad (3.3)$$

$$Q_1 = \frac{XV_1{}^2 - XV_1V_2\cos\delta - RV_1V_2\sin\delta}{R^2 + X^2} \qquad (3.4)$$

Where:

$\bar{S}_1$ is the complex power supplied by the inverter.

P_1 is the real power supplied by the inverter.

Q_1 is the reactive power supplied by the inverter output.

$V_1 \llcorner \delta$ is the output voltage of the inverter and δ is the phase angle of the output voltage of the inverter with respect to the grid.

$V_2 \llcorner 0°$ is the grid voltage.

$\bar{I}$ is the line current flowing from the inverter to the utility grid.

$\bar{Z} = R + jX$ is the line impedance.

As mentioned above, the grid power is found by three different methods.

Method 1- $\bar{S} = \bar{I}\bar{V}$:

$$\bar{S}_2 = P_2 + jQ_2 = \bar{V}_2 \bar{I}^* \qquad (3.5)$$

$$\bar{I} = \frac{\bar{V}_1 - \bar{V}_2}{R + jX}$$

$$\bar{S}_2 = \frac{RV_1V_2 cos\delta + XV_1V_2 sin\delta - RV_2^2 + jXV_1V_2 cos\delta - jRV_1V_2 sin\delta - jXV_2^2}{R^2 + X^2}$$

$$P_2 = \frac{RV_1V_2 cos\delta + XV_1V_2 sin\delta - RV_2^2}{R^2 + X^2} \qquad (3.6)$$

$$Q_2 = \frac{XV_1V_2 cos\delta - RV_1V_2 sin\delta - XV_2^2}{R^2 + X^2} \qquad (3.7)$$

Where:

$\bar{S}_2$ is the complex power absorbed by the grid.

P_2 is the real power absorbed by the grid.

Q_2 is the reactive power absorbed by the grid.

Method 2- Gauss-Seidel:

In order to find the power using power flow methods, the Y_{matrix} has to be found as following:

$$\bar{Z} = R + jX \; ; Y = \frac{1}{\bar{Z}} = G + jB$$

Building the Y_{matrix}:

$$Y = \begin{bmatrix} -(G + jB) & G + jB \\ G + jB & -(G + jB) \end{bmatrix}$$

$$\bar{Y}_{12} = \bar{Y}_{21}; \; \bar{Y}_{11} = \bar{Y}_{22}$$

$$\bar{Y}_{12} = -\bar{Y}_{22}$$

Now, the Y_{matrix} is used to calculate the power:

$$P_2 - jQ_2 = \bar{V}_2^* \sum_{i=1}^{n=2} Y_{i2}\bar{V}_i$$

$$P_2 - jQ_2 = Y_{12}V_2V_1\llcorner\delta + Y_{22}V_2{}^2$$

$$P_2 - jQ_2 = \left(V_2V_1\llcorner\delta - V_2{}^2\right)(G + jB)$$

$$P_2 - jQ_2 = \frac{V_2V_1\llcorner\delta - V_2{}^2}{R + jX}$$

$$P_2 - jQ_2 = \frac{V_2V_1\cos\delta + V_2V_1\sin\delta - V_2{}^2}{R + jX} \times \frac{R - jX}{R - jX}$$

$$P_2 - jQ_2 = \frac{RV_1V_2\cos\delta + XV_1V_2\sin\delta - RV_2{}^2 - jXV_1V_2\cos\delta + jRV_1V_2\sin\delta + jXV_2{}^2}{R^2 + X^2}$$

$$P_2 = \frac{RV_1V_2\cos\delta + XV_1V_2\sin\delta - RV_2{}^2}{R^2 + X^2} \qquad (3.6)$$

$$Q_2 = \frac{XV_1V_2\cos\delta - RV_1V_2\sin\delta - XV_2{}^2}{R^2 + X^2} \qquad (3.7)$$

Method 3- Newton-Raphson:

$$P_2 + jQ_2 = \bar{V}_2 \sum_{i=1}^{n=2} \bar{Y}_{i2}{}^*\bar{V}_i{}^*$$

22

The same Y_{matrix} calculated in the Gauss-Siedel method is used.

$$P_2 + jQ_2 = \bar{Y}_{12}{}^* \bar{V}_2 \bar{V}_1{}^* + \bar{Y}_{22}{}^* V_2{}^2$$

Since $\bar{Y}_{12} = -\bar{Y}_{22} \Rightarrow \bar{Y}_{12}{}^* = -\bar{Y}_{22}{}^*$

Therefore,

$$P_2 + jQ_2 = (\bar{V}_2 \bar{V}_1{}^* - V_2{}^2)\bar{Y}_{12}{}^*$$

$$P_2 + jQ_2 = \frac{V_2 V_1 \cos\delta - V_2 V_1 \sin\delta - V_2{}^2}{R - jX} \times \frac{R + jX}{R + jX}$$

$$P_2 - jQ_2 = \frac{RV_1 V_2 \cos\delta + XV_1 V_2 \sin\delta - RV_2{}^2 + jXV_1 V_2 \cos\delta - jRV_1 V_2 \sin\delta - jXV_2{}^2}{R^2 + X^2}$$

$$P_2 = \frac{RV_1 V_2 \cos\delta + XV_1 V_2 \sin\delta - RV_2{}^2}{R^2 + X^2} \qquad (3.6)$$

$$Q_2 = \frac{XV_1 V_2 \cos\delta - RV_1 V_2 \sin\delta - XV_2{}^2}{R^2 + X^2} \qquad (3.7)$$

The three methods give the same real and reactive power equations.

3.2 Effects of the Inputs of the System on the Power

The performance of the system under certain effects of some inputs is tested by implementing the power equations (3.3, 3.4, 3.6, and 3.7) in MATLAB. The need of studying the system performance is to recognize how a certain input impacts the generated power. The way implementations are processed is by varying a specific input and fixing the other inputs. The values of the equations' parameters are shown in Table 3.1.

Table 3.1: The parameters of the mathematical model

Output voltage of the inverter(V_1)	1
The grid voltage(V_2)	1
Reactance of the line impedance(X)	1
Resistance of the line impedance(R)	0 - 7
The phase of output voltage of the inverter(δ)	0°- 180°

The effects of the line resistance (R), the phase angle of power (δ), and the inverter output voltage (V_1) on the inverter power are shown below.

1. P_1 & Q_1 vs. R:

The power equations for the inverter are plotted for δ= 90° and other parameters are shown in Table 3.1.
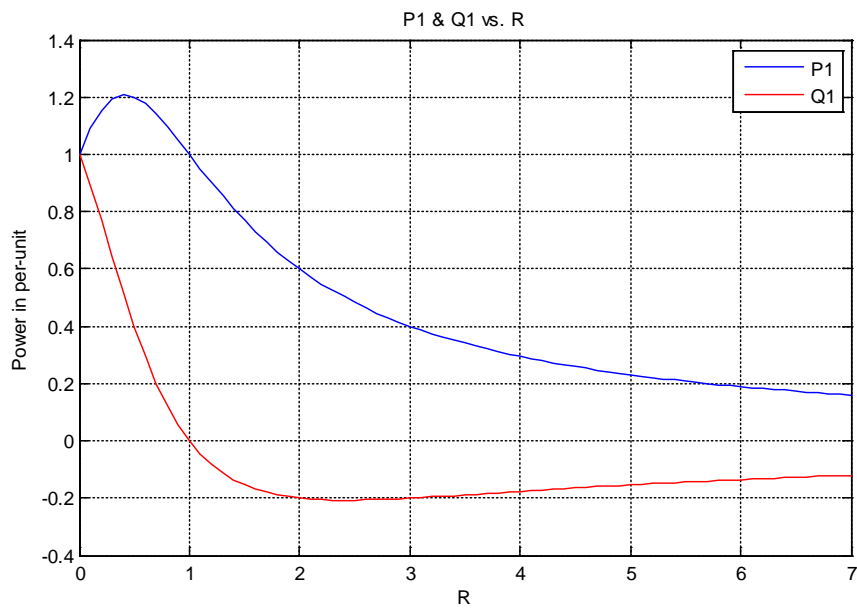
Fig. 3.2: The inverter real and reactive power versus the line resistance.

The figure shows that real power increases slightly until R is less than 0.5. Then it decreases as R increases and goes to zero. The reactive power is decreased sharply by increasing R. Then, the reactive power increases slightly and it goes to zero.

2. P_1 & Q_1 vs. δ:

δ varies from 0° t0 180°, and R/X is equal to 1.

Fig. 3.3: The inverter real and reactive power versus δ.

From Fig. 3.3, both real power and reactive power are shifted up and the peak value is increased.

3. P_1 & Q_1 vs. V_1:

V_1 varies from 0.9 to 1 and V_2 is 1. δ is set at 45° and R/X is set to be 1.

Fig. 3.4: The inverter real and reactive power versus the inverter output voltage.

The graph shows that real power and reactive power are increased constantly as V_1 increases.

Additionally, the effects of the three parameters (R, δ, and V_1) on the grid real power and reactive power are shown below.

1. P_2 & Q_2 vs. R:

X is set to be 1 and δ is 90°. Fig. 3.5 shows that the real power is decreased as R increases until it becomes steady. The reactive power is decreased sharply by increasing R from 0 to 0.7. From a certain value of R, the reactive power increases gradually until it becomes steady at zero.
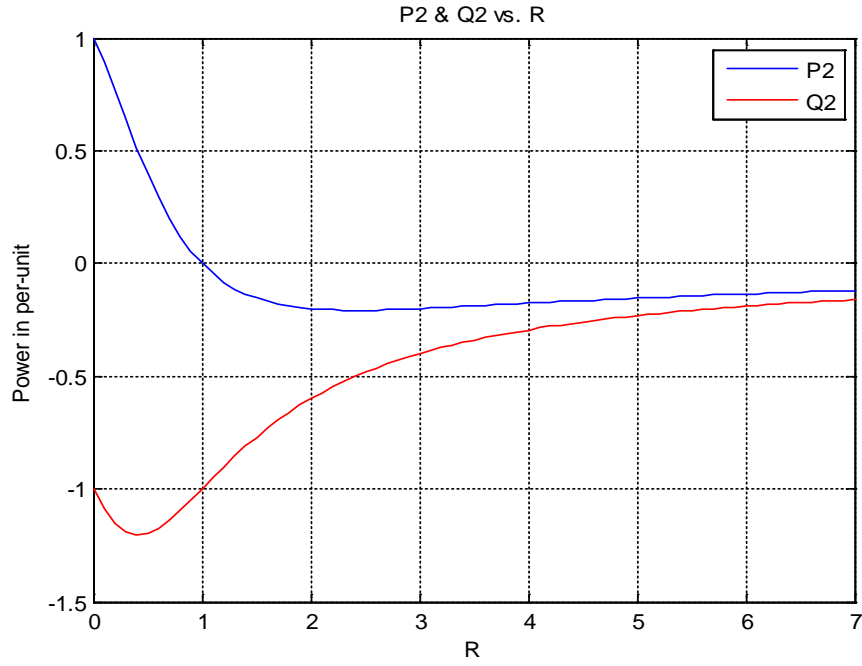
Fig. 3.5: The grid real and reactive power versus line resistance.

2. P_2 & Q_2 vs. δ:

δ varies from 0° to 180°, and R/X is equal to 1.
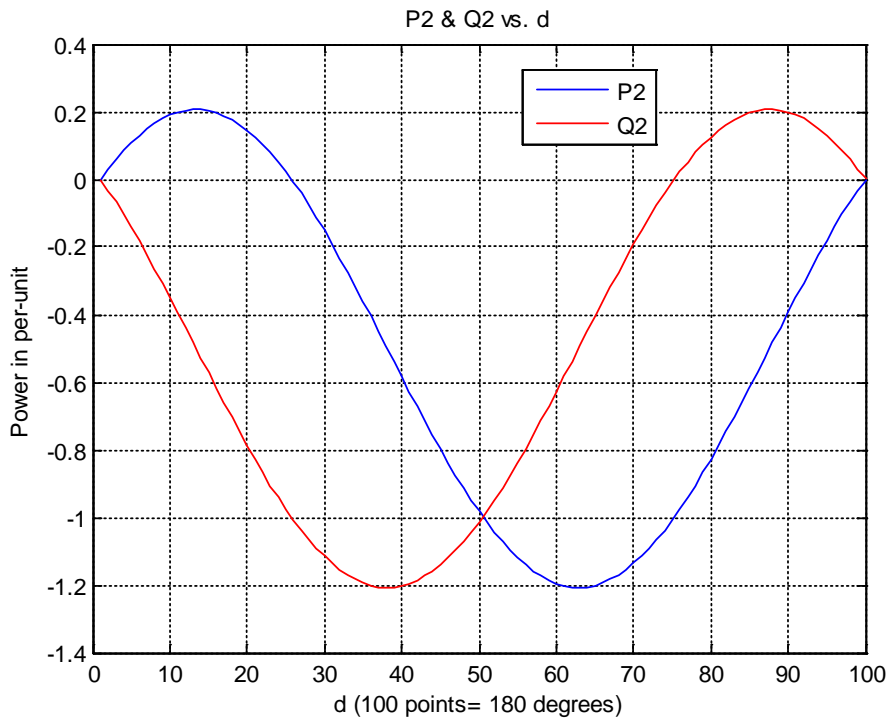
Fig. 3.6: The grid real and reactive power versus δ.

Fig. 3.6 shows that the real power and the reactive power are shifted down, so the peak values are decreased.

3. P_2 & Q_2 vs. V_1:

V_1 varies from 0.9 to 1 and V_2 is 1. δ is set to be 45° and R/X is set at 1.

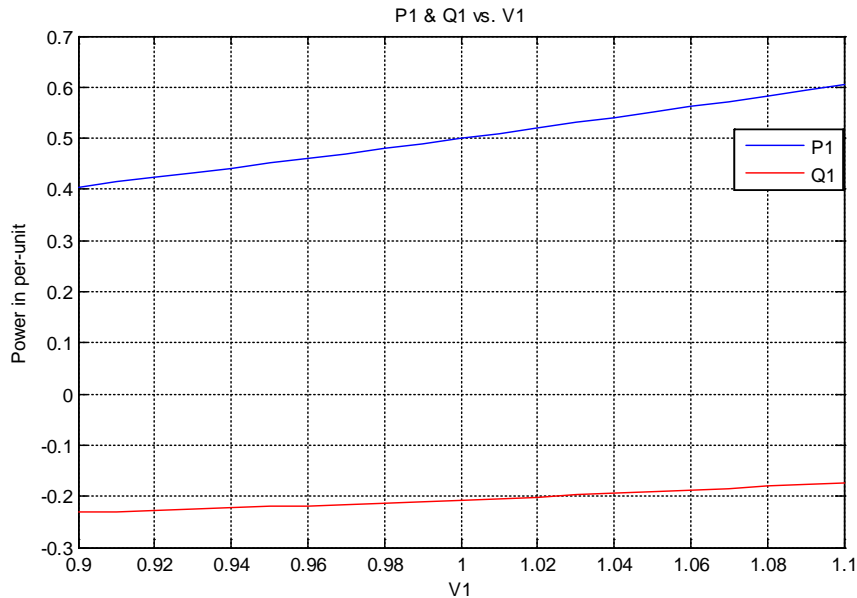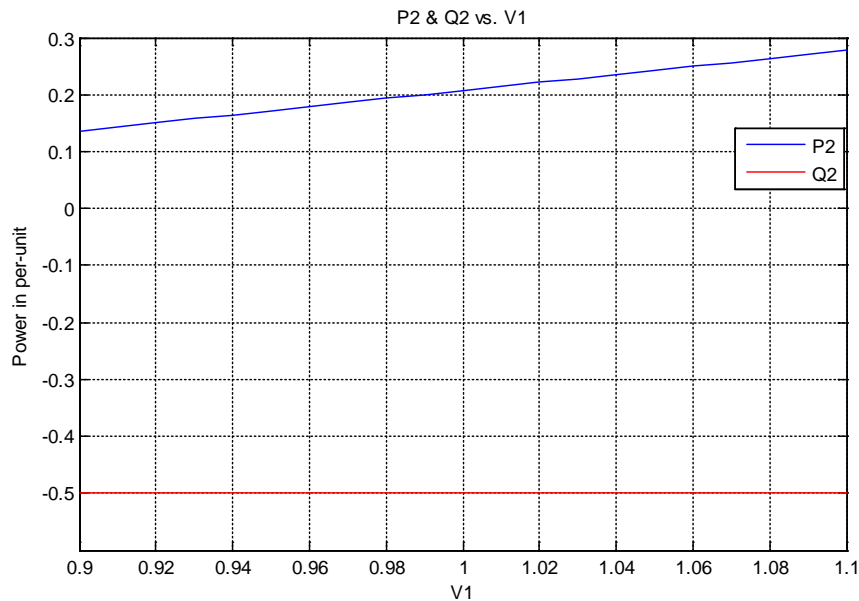

Fig. 3.7: The inverter real and reactive power versus the inverter output voltage.

The graph shows that the real power increases constantly by increasing V_1. The reactive power is steady at -0.5 as V_1 varies

The effects of R, δ, and V_1 on the active power of the system can be summarized in three points:

1. The power decreases when R/X increases.

2. The variation of δ impacts the real and reactive power from the inverter and the real and the reactive power at the grid.

3. The real and reactive power from the inverter increases by increasing V_1. The grid real power increases with increasing V_1, but the reactive power is steady.

3.3 Sensitivity Analysis of the Power

The study of system sensitivity is necessary in order to build a proper control system [19]. It is aimed to test the effects of system input variations on the output and examine the system reactions in response to these variations [19] [20]. Since this research focuses on the line impedance, the influence of the line impedance on the power and its effects on the system are studied. The effects of system inputs are different because the output is more affected by specific inputs than others. In other words, some inputs are more dominant than others. Moreover, studying the sensitivity of power helps in determining the maximum power [20].

The sensitivity of real and reactive power is examined by deriving the first derivative of the real and reactive power equations with respect to the parameters of line impedance:R and X. All equations are simulated and plotted using MATLAB.

3.3.1 Sensitivity of the inverter power

In this part, the first derivative of equations (3.3) and (3.4) is calculated with respect to R and X.

1. $\dfrac{\partial P_1}{\partial R}$ & $\dfrac{\partial Q_1}{\partial R}$:

$$\frac{\partial P_1}{\partial R} = \frac{R^2 V_1 V_2 cos\delta - R^2 V_1{}^2 - X^2 V_1 V_2 cos\delta + X^2 V_1{}^2 - 2XRV_1 V_2 sin\delta}{(R^2 + X^2)^2} \qquad (3.8)$$

$$\frac{\partial Q_1}{\partial R} = \frac{R^2 V_1 V_2 sin\delta - X^2 V_1 V_2 cos\delta - 2XRV_1 V_2 cos\delta + 2XRV_1{}^2}{(R^2 + X^2)^2} \qquad (3.9)$$

Both equations (3.8 and 3.9) are implemented where $V_1 = V_2 = 1$, X= 1, and δ= 90°.
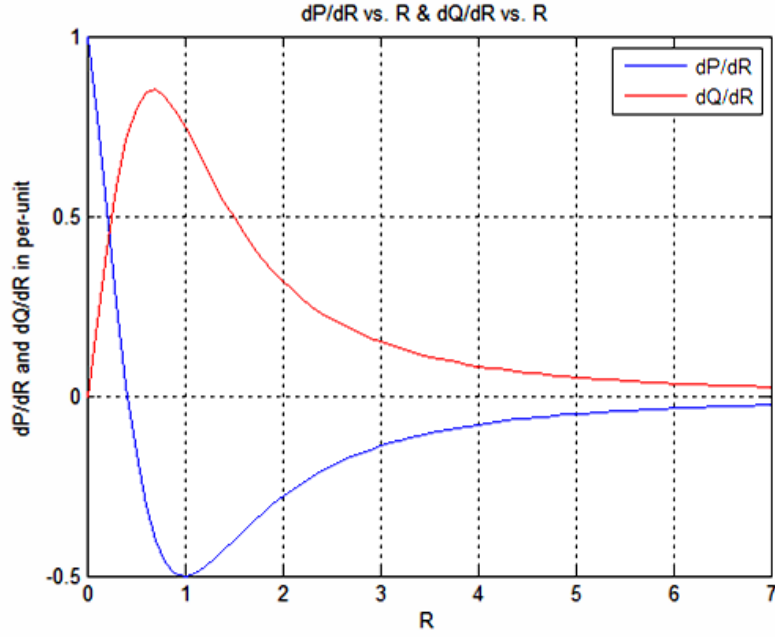
Fig. 3.8: dP1/dR and dQ1/dR versus the line resistance.

The figure shows that the partial derivative of the real power with respect to R goes down sharply and then it increases gradually until it becomes steady. Then, it increases until a certain value of R, and, then it becomes steady. Both partial derivatives of the real and reactive power become stable with increasing resistance.

2. $\dfrac{\partial P_1}{\partial X}$ & $\dfrac{\partial Q_1}{\partial X}$:

$$\frac{\partial P_1}{\partial X} = \frac{R^2 V_1 V_2 \sin\delta - X^2 V_1 V_2 \sin\delta + 2XRV_1 V_2 \cos\delta - 2XRV_1{}^2}{(R^2 + X^2)^2} \qquad (3.10)$$

$$\frac{\partial Q_1}{\partial X} = \frac{R^2 V_1{}^2 + X^2 V_1 V_2 \cos\delta - R^2 V_1 V_2 \cos\delta - X^2 V_1{}^2 + 2XRV_1 V_2 \sin\delta}{(R^2 + X^2)^2} \qquad (3.11)$$

Both equations (3.10 and 3.11) are implemented where $V_1 = V_2 = 1$, R= 1, and δ= 45°.
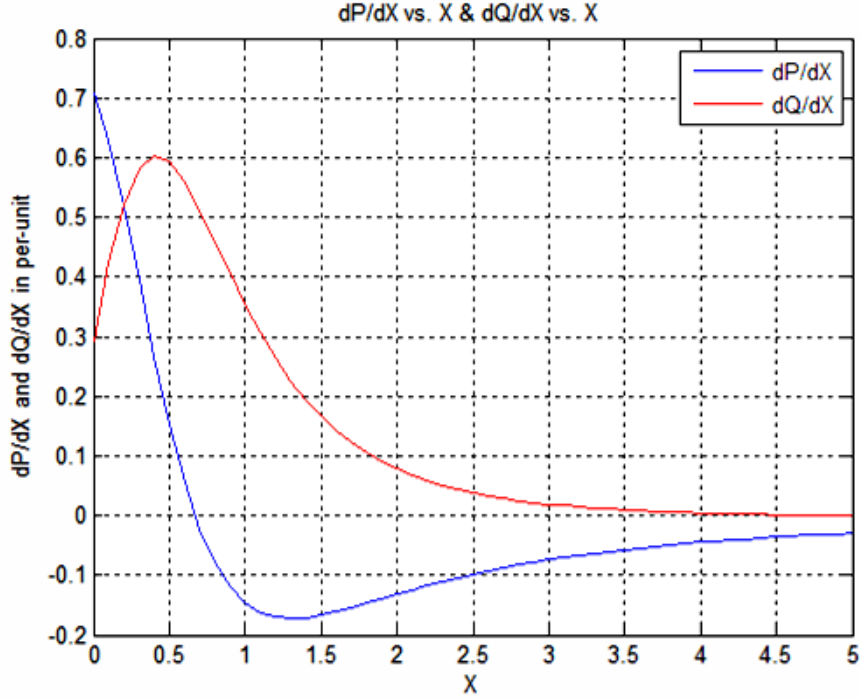
Fig. 3.9: dP_1/dX and dQ_1/dX versus the line reactance.

The figure shows that the partial derivative of the real power with respect to X decreases sharply and then it increases slightly until it becomes stable. The partial derivative of the reactive power with respect to X goes up until X=0.4 and then it goes down until it becomes steady at zero when X equals about 4.5.

3.3.2 Sensitivity of the grid power

In this part, the first derivative of equations (3.6) and (3.7) is calculated with respect to R and X.

1. $\frac{\partial P_2}{\partial R}$ & $\frac{\partial Q_2}{\partial R}$:

$$\frac{\partial P_2}{\partial R} = \frac{R^2 V_2^2 - R^2 V_1 V_2 \cos\delta + X^2 V_1 V_2 \cos\delta - X^2 V_2^2 - 2XRV_1 V_2 \sin\delta}{(R^2 + X^2)^2} \qquad (2.12)$$

$$\frac{\partial Q_2}{\partial R} = \frac{R^2 V_1 V_2 \sin\delta - X^2 V_1 V_2 \cos\delta - 2XRV_1 V_2 \cos\delta + 2XRV_2^2}{(R^2 + X^2)^2} \qquad (2.13)$$

Both equations (3.12 and 3.13) are implemented where $V_1 = V_2 = 1$, X= 1, and δ= 90°.
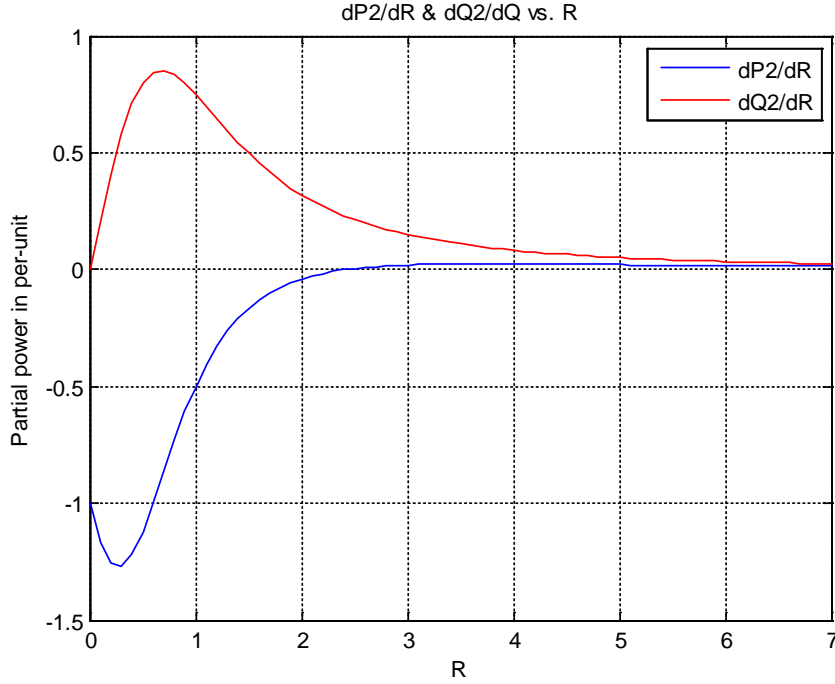
Fig. 3.10: dP2/dR and dQ2/dR versus the line resistance.

The figure shows that the partial derivative of the real power with respect to R decreases until R is about 0.3, then it increases exponentially until it becomes steady at zero. The partial derivative of the reactive power with respect to R increases as R increases. At a certain value of R, both curves becomes steady at zero.

2. $\dfrac{\partial P_2}{\partial X}$ & $\dfrac{\partial Q_2}{\partial X}$:

$$\frac{\partial P_2}{\partial X} = \frac{R^2 V_1 V_2 sin\delta + X^2 V_1 V_2 cos\delta - 2XRV_1 V_2 cos\delta - 2X^2 V_1 V_2 sin\delta + 2XRV_2{}^2}{(R^2 + X^2)^2} \qquad (3.14)$$

$$\frac{\partial Q_2}{\partial X} = \frac{X^2 V_2{}^2 + R^2 V_1 V_2 cos\delta - X^2 V_1 V_2 cos\delta - R^2 V_2{}^2 + 2XRV_1 V_2 sin\delta}{(R^2 + X^2)^2} \qquad (3.15)$$

Both equations (3.8 and 3.9) are implemented where $V_1=V_2=1$, R= 1, and δ= 45°. Fig. 3.11 shows that the partial derivative of the real power with respect to X decreases sharply, then it increases slightly until it becomes steady at zero. The partial derivative of the reactive power with respect to X increases sharply from X= 0 to X=

32

0.8. Then it decreases gradually until it becomes steady. Both curves are going to be stable for larger X.
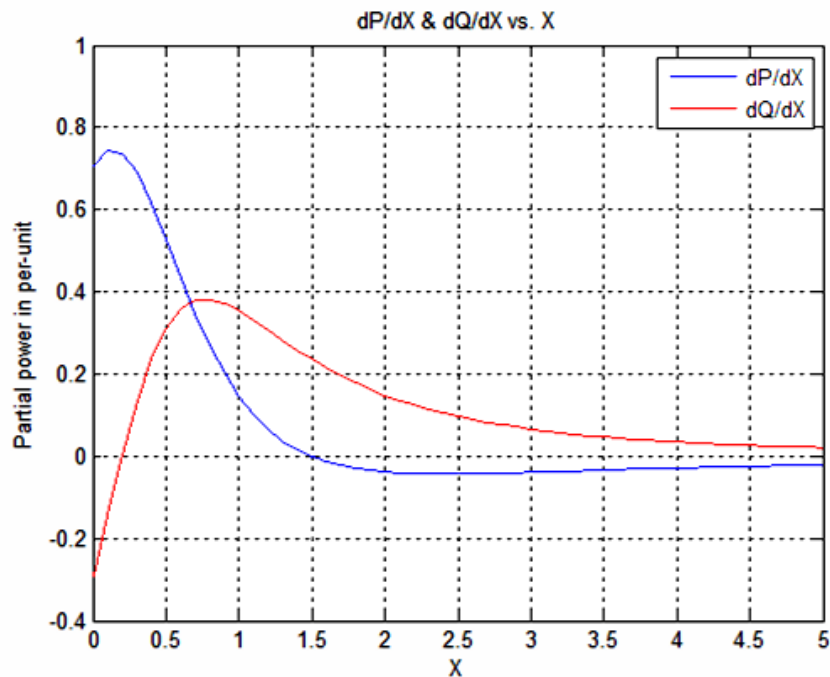
Fig. 3.11: dP2/dX and dQ2/dX versus the line reactance.

After studying the sensitivity of power to the line impedance, the power is certainly affected by the line impedance. Each parameter of the line impedance has its own amount of effect on the power.

3.4 Circuit Modeling of the Grid-connected PV System

The proposed system is modeled using SIMPLIS to collect simulation results and plot them using MATLAB. The model is built step by step. First, the inverter is built using four voltage controlled switches, four diodes, and a DC voltage source representing PV panels. The inverter is connected to two loads, one of which is resistive and the other is resistive and inductive, to verify the operation of the inverter. Second, the voltage sources controlling the switches are replaced with sinusoidal pulse width modulation (SPWM) control signals to control the switches. Then, an LC

filter is designed in order to get rid of unwanted components in the output voltage or current. Finally, the inverter is connected to an AC voltage source representing the grid voltage. The circuit is modeled and simulated using SIMPLIS.

3.4.1 SIMPLIS Software

SIMPLIS is the selected program to model and analyze the grid-connected PV system in this thesis. SIMPLIS is a simulation program for integrated circuits [21]. The performance of electronic circuits is simulated in SIMPLIS to let designers examine their circuits before circuit construction. In SIMPLIS, the designer can use piecewise linear (PWL) analysis and modeling techniques which means the system is a linear network. Also, SIMPLIS has a very fast transient simulation, 10 to 50 times faster than PSpice.

3.4.2 The inverter Model

The initial model of the inverter in this research consists of four ideal switches controlled by four ac voltage sources of frequency of 60 Hz and four ideal diodes. The topology of the inverter is a basic single phase full bridge inverter. Fig. 3.12 shows the basic inverter model. The switches and diodes are ideal with switching frequency of 60 Hz. The DC source is 120 V. An arbitrary load is picked to examine the inverter output. The load has a resistance of 20 Ω.
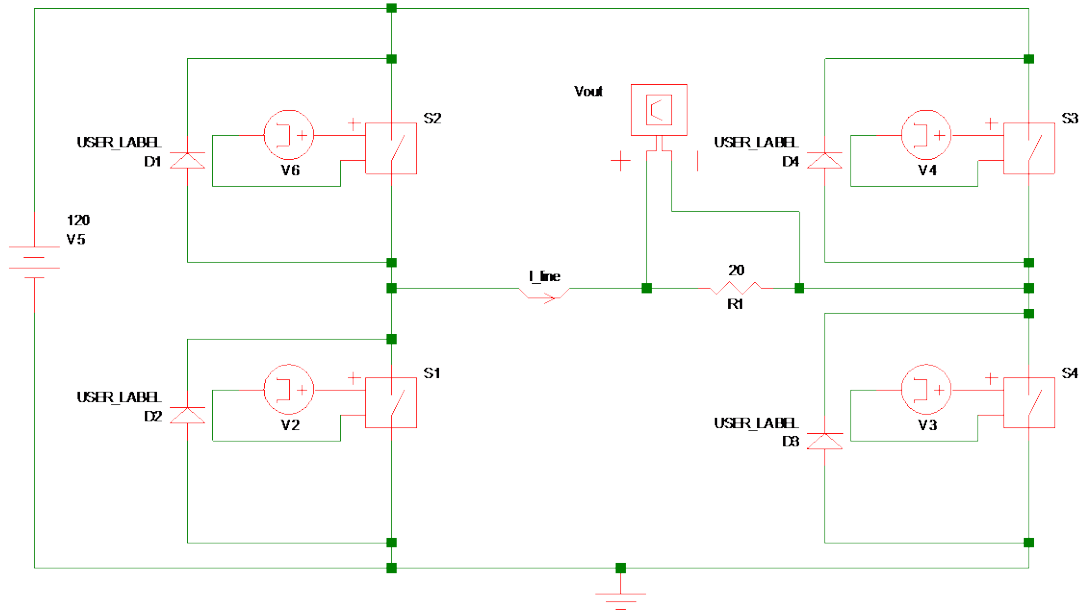
Fig. 3.12: The inverter with resistive load.

time/mSecs   5mSecs/div
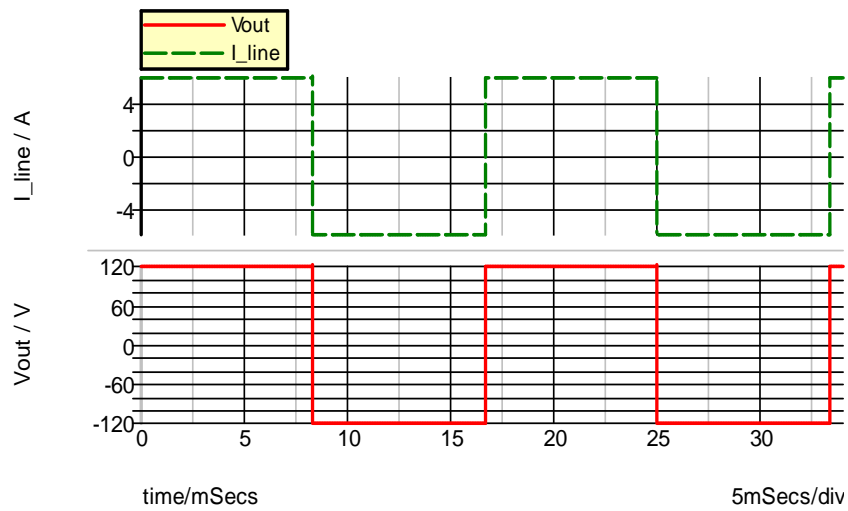
Fig. 3.13: The inverter outputs.

The graph shows that the amplitude current is equal to 6 A. We can check that from Ohm's law:

$$I = \frac{V}{R} \qquad (3.16)$$

$$I = \frac{120}{20} = 6 \, A$$

35

The plots also show that the frequency is 60 Hz, because the voltage sources control the switches are set at frequency of 60 Hz. The total harmonic distortion (THD) of both outputs is 46.6%

An inductive load of 100 mH is added to the load. The effect of inductance on the current is shown in Fig. 3.15. THD is measured, and it is 46.6% for the output voltage and 12.3% for the current.
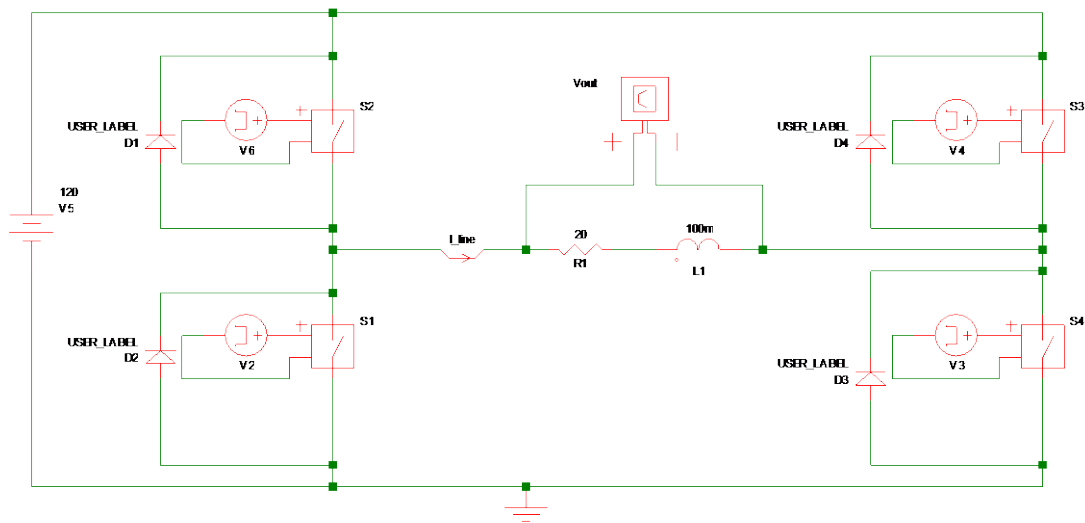
Fig. 3.14: Inverter with RL load.
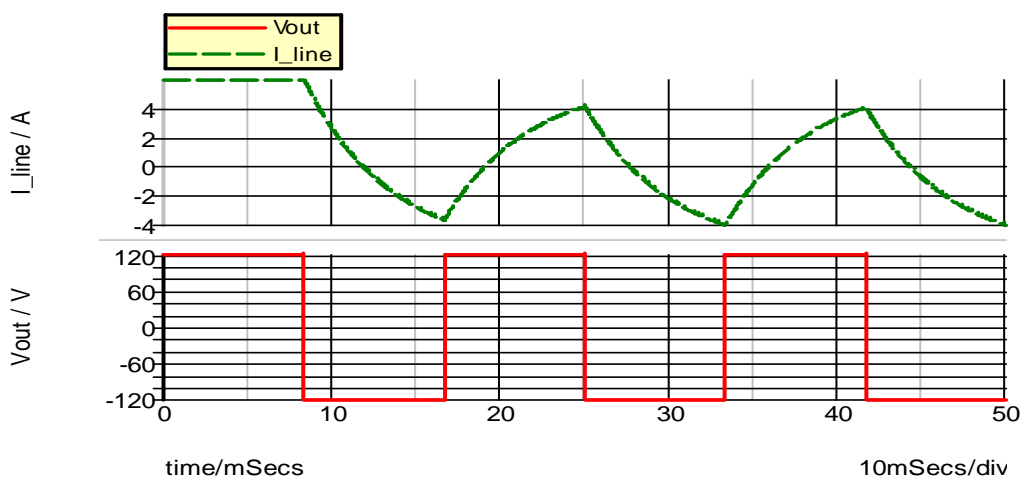
Fig. 3.15: The output current and voltage of the inverter.

2.4.3 The Design of SPWM

Pulse width modulation (PWM) is a method where the output frequency and voltage can be controlled by switched voltage pulses [22]. PWM has several advantages such as decreasing the harmonic distortion of load current, reducing switching losses, tracking the phase and the frequency of the grid, improving the efficiency, fast voltage regulation, and providing fast tuning rate [14][22-25]. PWM has different schemes: SPWM, hysteresis PWM (HPWM), space vector modulation (SVM), and optimal PWM [18]. SPWM and HPWM are universally common in PV applications. For that reason, SPWM is utilized here.

The four voltage sources controlling the switches are replaced by a circuit to generate SPWM signals. The circuit consists of two wave generators, one of which is the control signal and the other is the carrier signal [26]. The control signal is a sinusoidal wave, and its frequency is set to the desired frequency 60 Hz. The carrier signal is a triangular wave. It always has a higher frequency than that of the control signal. The modulation index is defined as the ratio of the amplitude of the control signal over the amplitude of the triangular wave:

$$m_a = \frac{V_c}{V_t} \quad ; \quad 0 \le m_a \le 1 \qquad (3.17)$$

where m_a is the modulation index, V_c is the amplitude of the control signal and V_t is the amplitude of the triangular signal. In the interest of this research, the SPWM voltages are chosen where V_c is 1 V and V_t is 1 V. Also, frequency modulation is defined as the division of the frequency of the triangular signal over the frequency of the control signal.

$$m_f = \frac{f_t}{f_s} \qquad m_f \ge 1 \qquad (3.18)$$

The variable definitions are defined where m_f is the modulation ratio, f_s is the frequency of the control signal and f_t is the frequency of the triangular signal. The desired frequency is 60 Hz. The switching frequency being picked is $f_t = 9.9\ kHz$, because the high switching frequency of PWM shifts the unwanted harmonics of the unfiltered signal to the switching frequency. The value of f_t is selected to obtain odd integer multiple of m_f in order to eliminate the odd-order harmonics and the harmonics are shifted to higher frequencies [27]. Therefore, m_a is equal to 1 and m_f is equal to 165.

The components needed to generate a sinusoidal PWM (SPWM) are:

1. Control signal -sinusoidal wave generator of frequency of 60 HZ.
2. Carrier signal, triangular wave generator of frequency of 9.9 kHz.
3. Comparator.
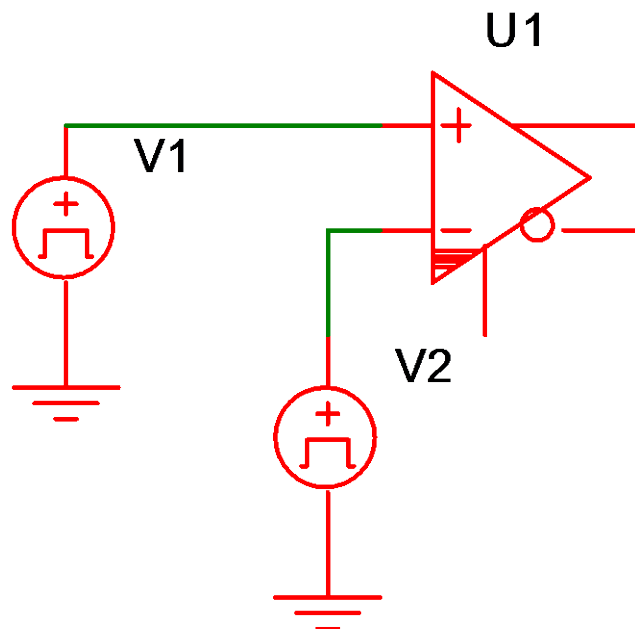
Fig. 3.16: SPWM circuit.
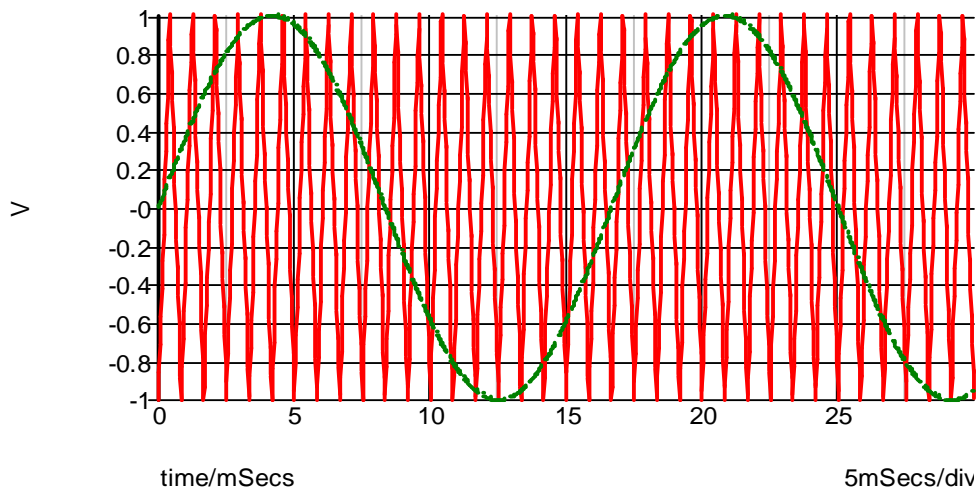
(a)
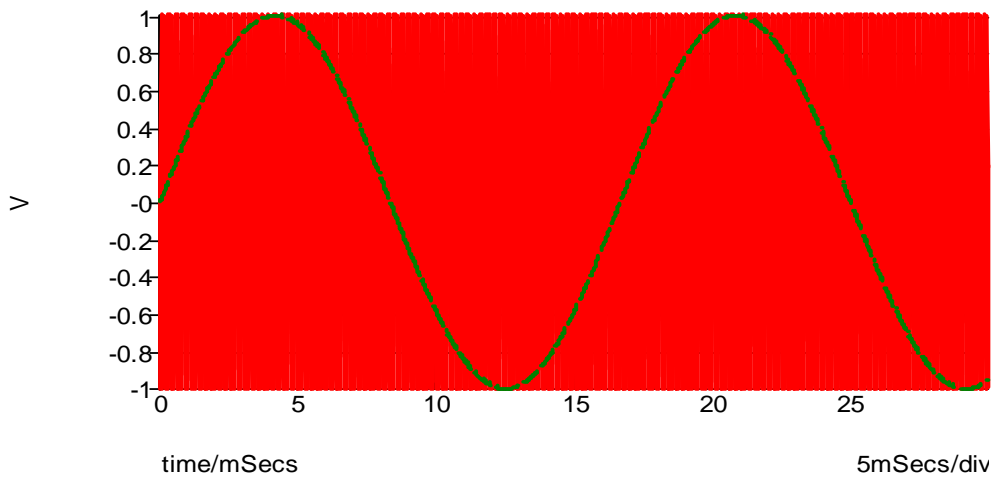
(b)

Fig. 3.17: (a) The output voltage of the control signal (sinusoidal) and the output voltage of the carrier signal (triangle) when m_f= 20. (b) The output voltage of the control signal (sinusoidal) and the output voltage of the carrier signal (triangle) when m_f= 165.
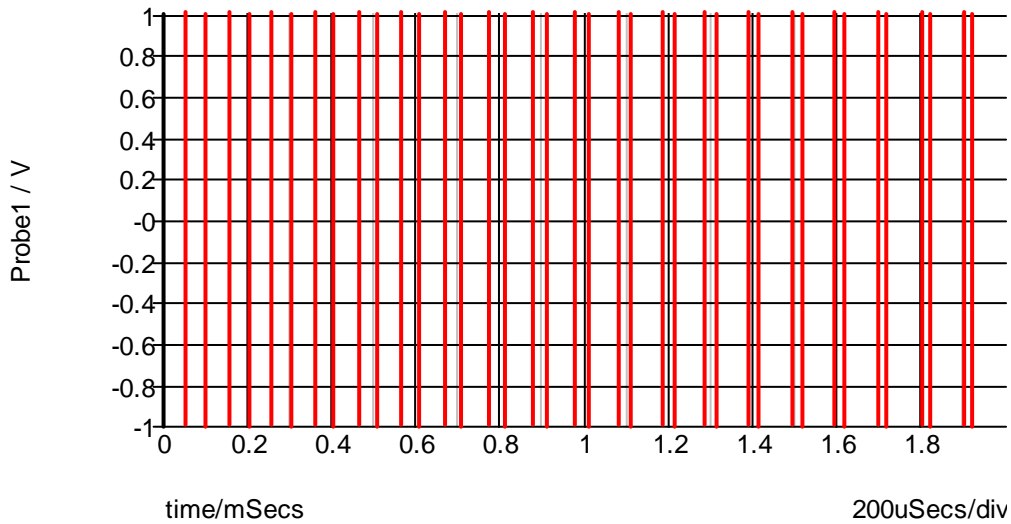
Fig. 3.18: The output signal after the control signal and the carrier signal compared through the comparator.

The switching sequence is simply that S1 and S4 are turned on and off together and the same with S2 and S3. When S1 and S4 are on, then S2 and S3 are off and vice versa. This switching sequence is known as bipolar switching. Now, SPWM signals are connected to the inverter switches. The circuit and the outputs are shown in the following figures.
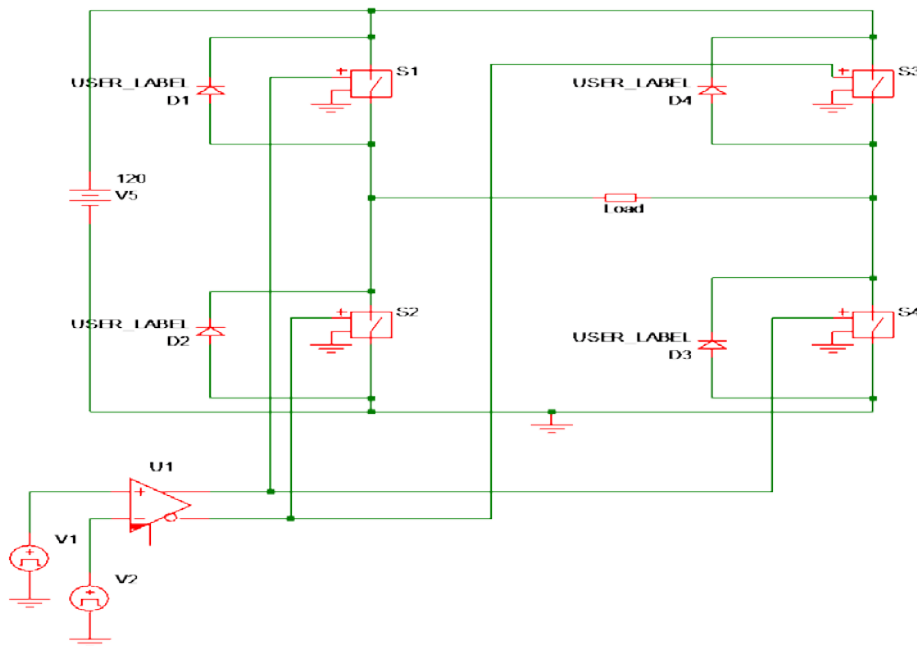
Fig. 3.19: SPWM Inverter.

40
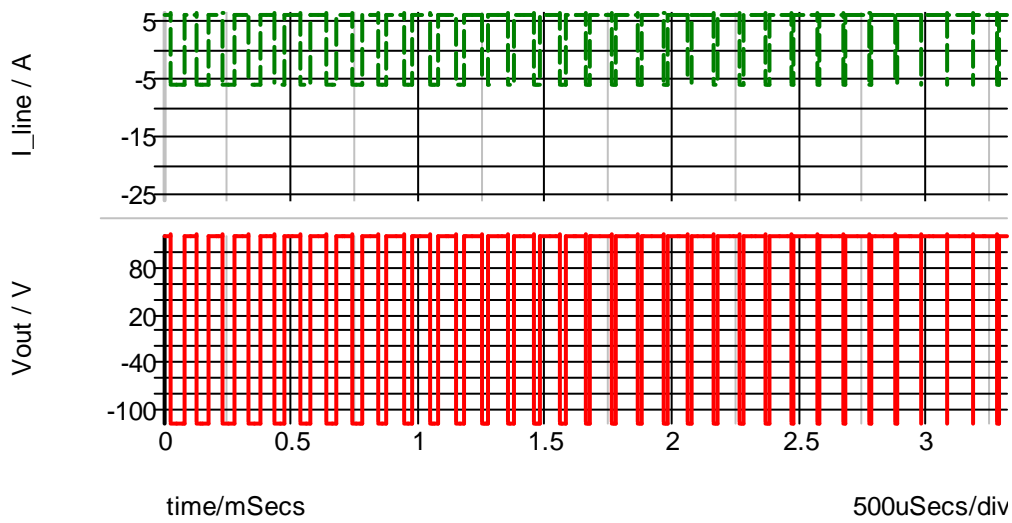
(a)
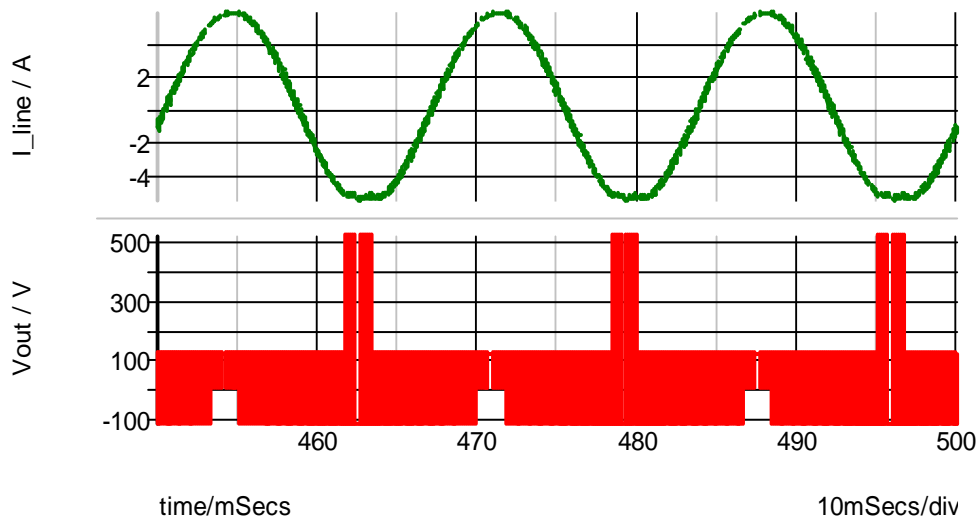
(b)

Fig. 3.20: (a) The output current and voltage when the load is resistive. (b) The

output current and voltage when the load is RL.

The output current in Fig. 3.20 (b) is a sinusoidal wave because of the inductance. The

outputs are distorted where the output voltage has THD of 107%. THD of the current

is THD of 1.7%. Therefore, a filter is needed to eliminate the harmonic distortion and

to make a pure sinusoidal wave.

41

3.4.4 Filter Design

A low-pass LC filter is designed to reduce the unwanted harmonics and to produce a high quality sinusoidal wave [22] [28]. Also, eliminating the ripple caused by switching requires a low cut-off frequency (f_c) and a high switching frequency [28]. For PWM, the high switching frequency shifts the unwanted harmonics of the unfiltered signal to the switching frequency as seen in Fig. 3.21. The SPWM here has a carrier frequency, switching frequency, of 9.9 kHz, and a control frequency of 60 Hz. To design the filter, the cut-off frequency has to be determined. However, it can be selected to be less than 9.9 kHz. For the design here, f_c is selected to be 1 kHz.
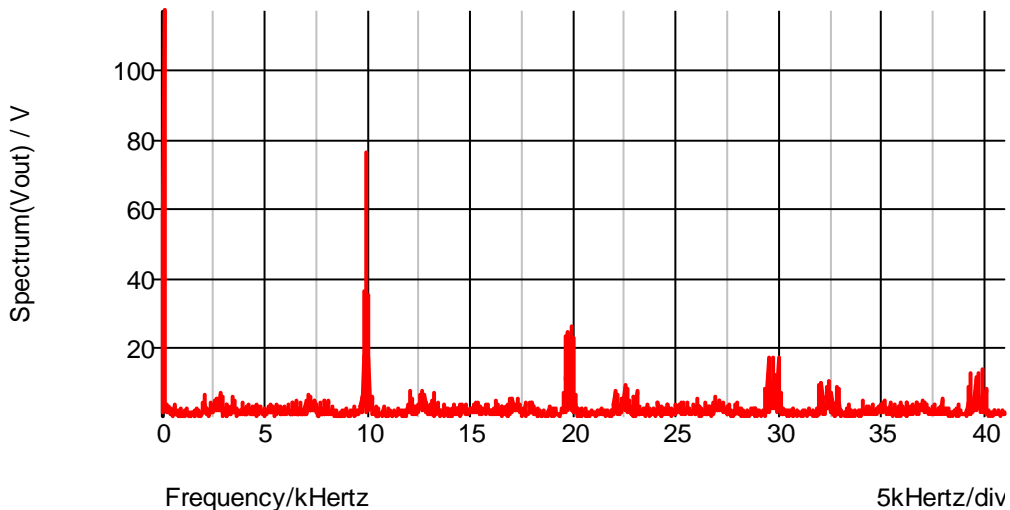
Fig. 3.21: Harmonic content of the inverter output voltage.

Assume $L_f = 100 \ \mu H$, the capacitor can be calculated from the following equation:

$$C_f = \frac{1}{(2\pi f_c)^2 L_f} \qquad\qquad (3.19)$$

So, C_f is equal to 253.3 μF.

42

Fig. 3.22: LC filter.

time/mSecs   10mSecs/div
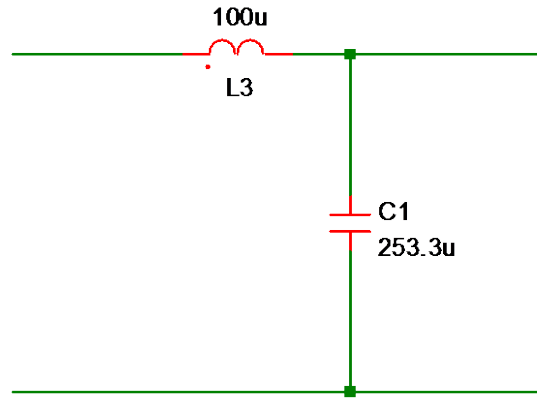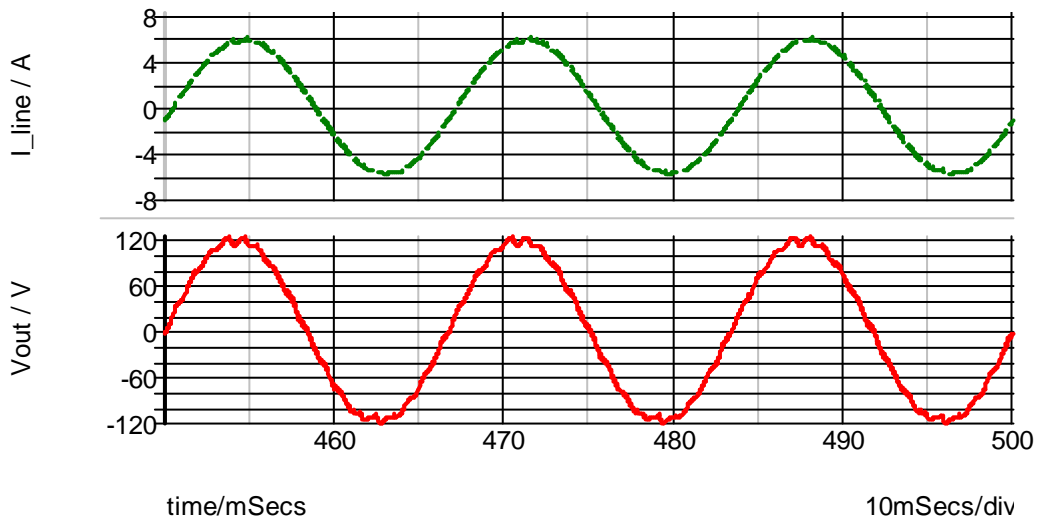
Fig. 3.23: The filtered line current and the output voltage.

The filter is added to the inverter circuit. Fig. 3.23 shows that the line current and the output voltage are sinusoidal with a frequency of 60 Hz. The current amplitude is still 6 A and the voltage amplitude is still 120 V. The output voltage has THD of 3.8% and the current has THD of 0.3%.

3.4.5 Connecting the Inverter to the Grid

The grid is modeled as a sinusoidal voltage source of amplitude of 120 V and frequency of 60 Hz. The line connecting the inverter with the grid has an impedance and is called the grid impedance. The complete model of the proposed grid-connected

PV system is shown in Fig. 3.24, and Fig. 3.25 shows the line current, the inverter output voltage, and the grid voltage.
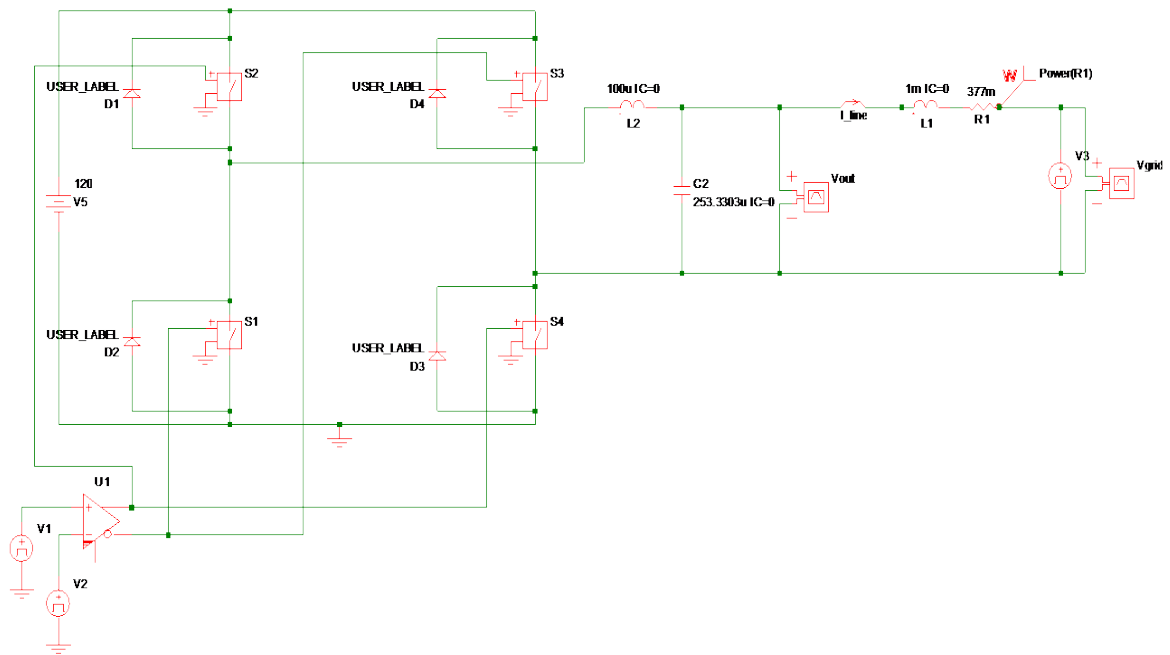
Fig. 3.24: The model of the grid-connected PV system.
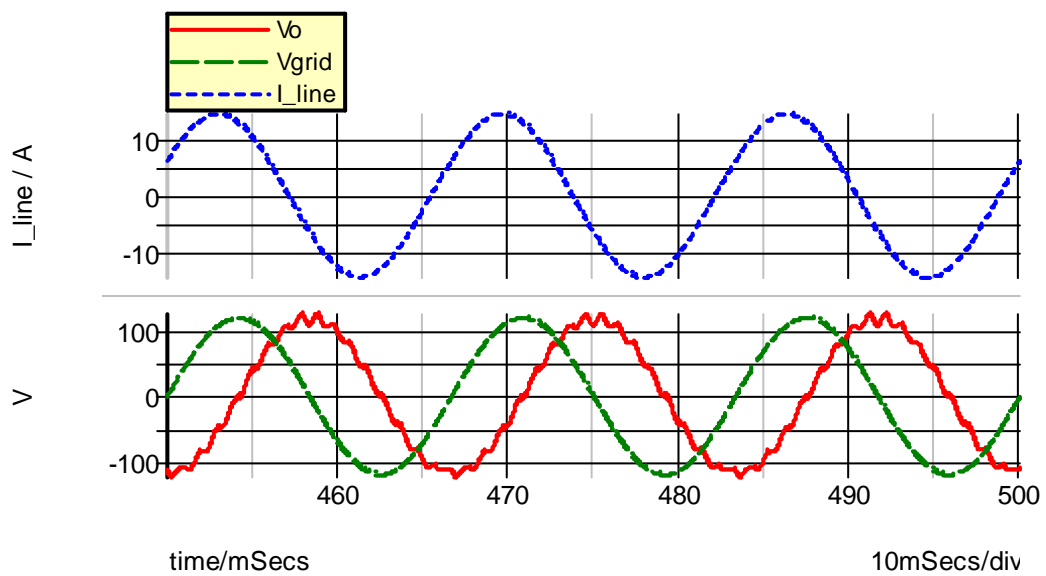
Fig. 3.25: The line current, the inverter output voltage, and the grid voltage.

4. Maximum Power Analysis under the Variations of R/X

The main aim of studying the effects of the grid resistance on real power is to determine the phase angle at which the power is at its maximum. The effects of R/X variations on real power are tested and analyzed. First, the current performance is examined at different R/X ratios from 0.5 to 7. The analysis is divided into two parts: theoretical analysis and experimental analysis. Then, four R/X ratios are selected to be tested for maximum power analysis. The value of the inductance is assumed fixed and the value of resistance is variable. After that, the power equations are implemented at the selected R/X ratios using MATLAB. Finally, the modeled circuit is simulated at the selected R/X ratios. The results of both models are compared.

4.1 The Effects of the Grid Resistance on the Line Current

The current from SIMPLIS is compared with calculation results of the current equation. The phase angle of the output voltage of the inverter is fixed at $0°$ in the first case and at $90°$ in the second case. The current is measured and plotted to see the impacts of varying R/X ratio. R and X values are shown in the following table.

Table 4.1: R/X ratio from 0.5 to 7

R/X	R(Ω)	X(Ω)
0.5	1.885	3.77
1	3.77	3.77
3	11.31	3.77
5	18.85	3.77
7	26.39	3.77

1. At $\delta= 0°$:

Table 4.2: The current at δ=0°

R/X	I_{peak}(mA)	Current plot

R/X	I_{peak}(mA)	Current plot
0.5	489	
1	416	
3	268	
5	203	

7	168	

The simulated current is supposed to be zero amperes, but, there is a numerical error in the SIMPLIS measurements. The current can be theoretically calculated from equation (3.2) as follows:

$$\bar{I} = \frac{\bar{V}_1 - \bar{V}_2}{R + jX}$$
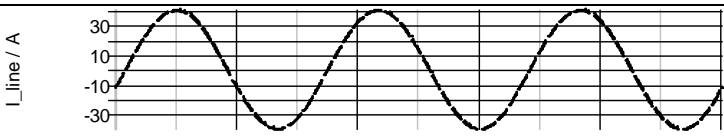
$$\bar{V}_1 - \bar{V}_2 = 120\llcorner 0° - 120\llcorner 0° = 0$$

$$\bar{I} = \frac{0}{R + jX} = 0\ A$$

For different R values, the current is equal to zero amperes. The simulated and theoretical currents are close.

2. At δ= 90°:

Table 4.3: The line current for δ=90°

R/X	I_{peak}(A)	Current and Power plots
0.5	40.52	

1	31.2	
3	14.21	
5	8.9	
7	6.4	
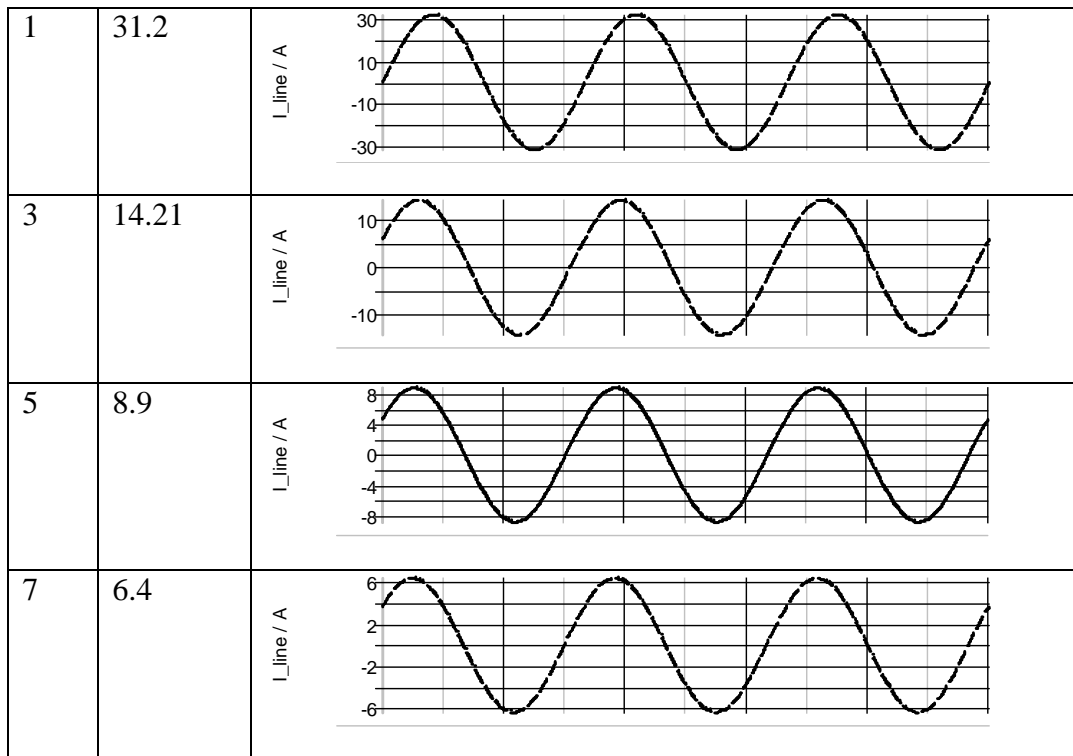
As seen from table 4.3, the current decreases as the resistance increases. Thus, the line resistance indeed affects the system and it has to be taken in account because it plays a significant role in the system.

In Table 4.4, the peak current is calculated theoretically and compared with the results from simulation in order to check that the simulation is working correctly.

Table 4.4: The theoretical and simulated current when δ=90°

R/X	Theoretical I_{peak}(A)	Simulated I_{peak}(A)	$E_{\%}$ of the Current
0.5	40.3	40.52	0.54%
1	31.83	31.2	1.9%
3	14.23	14.21	0.14%

5	8.83	8.9	0.79%
7	6.37	6.4	0.47%

From Table 4.4, the theoretical results and the experimental results are approximately equal.

4.2 Theoretical Analysis and Results

The theoretical analysis of the effects of the grid resistance on the maximum power transfer is studied using MATLAB. The power equations (3.3, 3.6) are implemented and plotted to find the maximum power phase angle for different R/X ratios. Per-unit is used in implementing the equations as shown in Table 4.5. The value of X and R used in the calculations are shown in the table.

Table 4.5: Parameters used to implement the power equations in MATLAB

V_1	1
V_2	1
X	1
R	0, 0.5, 1, and 3
Δ	0°- 180°

4.2.1 Maximum Power Calculations

Taking the first derivative of the real power of the grid with respect to δ yields the following:

$$P_2 = \frac{RV_1V_2cos\delta + XV_1V_2sin\delta - RV_2^2}{R^2 + X^2}$$

Set the derivative equal to zero to find the values of δ at which the real power is a maximum.

$$\frac{dP_2}{d\delta} = \frac{-Rv_1v_2sin\delta + Xv_1v_2cos\delta}{R^2 + X^2} = 0$$

$$-Rv_1v_2sin\delta + Xv_1v_2cos\delta = 0$$

$$Rv_1v_2sin\delta = Xv_1v_2cos\delta$$

$$Rsin\delta = Xcos\delta$$

$$\frac{sin\delta}{cos\delta} = \frac{X}{R}$$

$$tan\delta = \frac{X}{R} \qquad (4.1)$$

when $X \gg R$: $\delta = tan^{-1}(very\ large\ number) = 90°$

Therefore, the real power when R is zero is at its maximum at $\delta = 90°$. X/R is large for transmission lines, so the maximum power is approximately at $\delta = 90°$.

4.2.2 Maximum Power Simulation Results

For a distribution feeder, the X/R ratio is smaller. Therefore, the maximum power angle is changed by varying R/X. The effects of varying the R/X ratio on the maximum power are shown in Fig. 4.1.
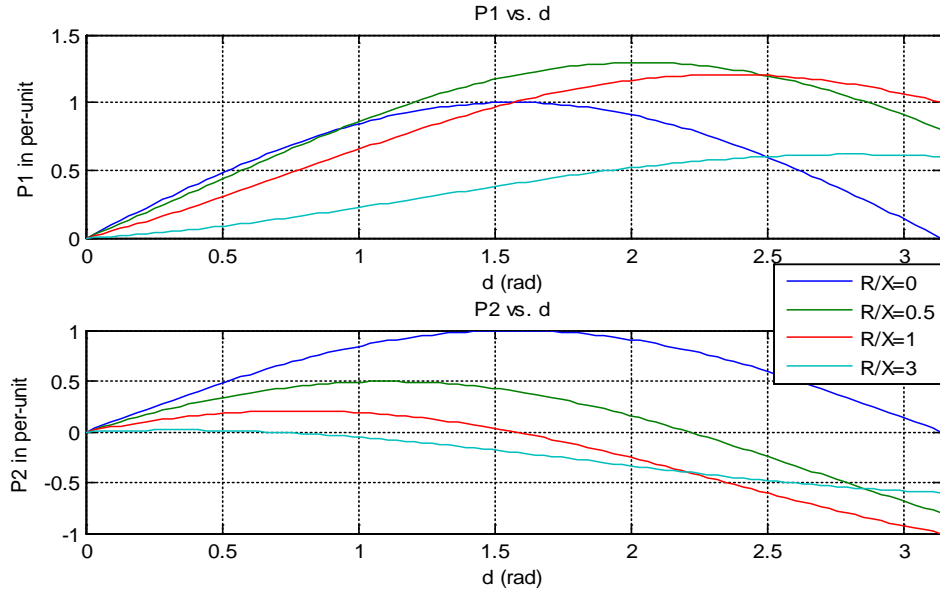
Fig. 4.1: The real power of the inverter and the real power of the grid for different

R/X ratios.

The maximum power angle of the grid is decreased by increasing the R/X ratio. And the maximum power angle of the output power from the inverter is increased as the R/X ratio increases. The amplitude of the grid power is decreased as the R/X ratio increases. The maximum power that can be transferred without losses is when R/X ratio is equal to 0. The figure can be interpreted in the next table.

Table 4.6: The phase angles for maximum power

R/X	$\delta_{P1,max}$	$\delta_{P2,max}$
0	90°	90°
0.5	116.36°	63.63°
1	134.54°	45.45°
3	161.82°	18.17°

The angle of maximum power of the grid decreases as the resistance increases, whereas for the power from the inverter, the phase angle increases as the resistance increases.

Additionally, the power at the grid and the power of the inverter when R/X is 0 is also calculated from the following equation:

$$P_1 = P_2 = \frac{V_1 V_2}{X} \sin(\delta) \qquad (4.2)$$

The circuit parameters are used to implement power equations as follows:

$V_1 = 120\ V$

$V_2 = 120\ V$

$X = 3.77\ \Omega.$

The maximum power is at $\delta = 90°$ because $\sin(90°) = 1$.

so,

$$P_{1,max} = P_{2,max} = 3819.83\ W$$

The power for different δ's is also calculated for comparison. The table shows the calculated power for several δ's.

Table 4.7: Power when R/X=0

δ	Power at the grid (W)
0°	0
30°	1909.8
45°	2700.9
60°	3307.9
90°	3819.83

Moreover, the power losses are plotted by subtracting the power equations (P_1-P_2).
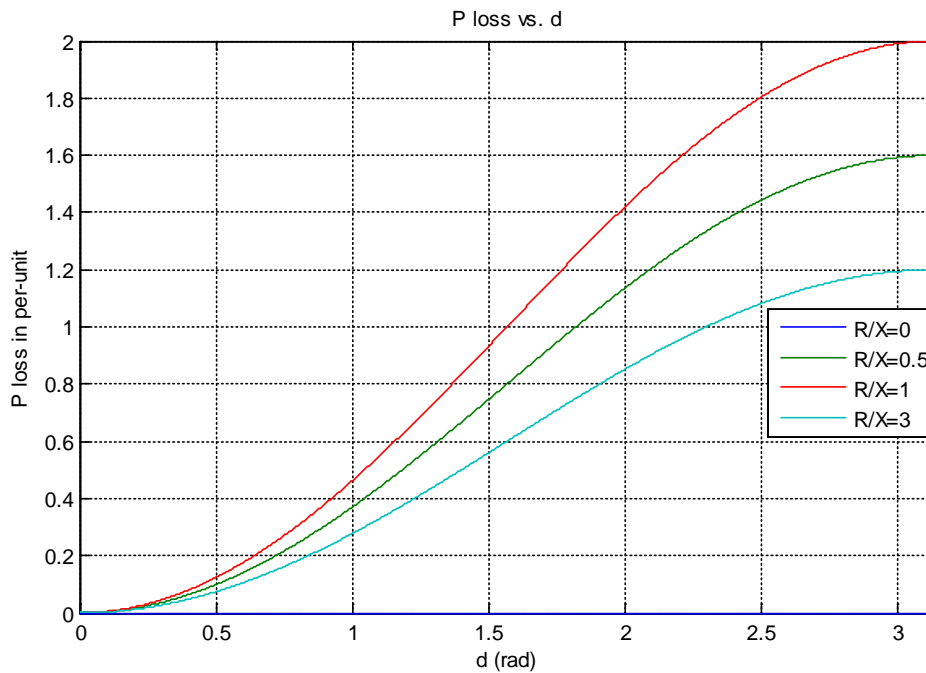
Fig. 4.2: Power losses for different R/X ratios.

There is no power loss at R/X= 0. The power losses increase as R/X increases. The losses increase as the angle of the output voltage of the inverter increases.

4.3 Simulation Analysis and Results

The circuit model was also simulated using SIMPLIS. SIMPLIS can determine the RMS value, mean value, maximum, frequency, and other measurements. Also, SIMPLIS has the ability to multiply the plotted curves. The same R/X ratios examined in the theoretical analysis are also tested in SIMPLIS in order to compare the results of both analyses. The power from the inverter and the grid power are measured by multiplying the current curve by the voltage curve. Then, the mean of the resultant plot of multiplied curves is measured. After that, the results are gathered and plotted

in MATLAB. The simulation results for power are shown in the following table. The data from the table is plotted as shown in Fig 4.3.

Table 4.8: (a) Power when R/X= 0.5. (b) Power when R/X= 1. (c) Power when R/X= 3.

	R/X= 0.5		
δ	$P_{1,avg}$ (W)	$P_{2,avg}$ (W)	P_{R_line} (W)
0°	-4.1	-4.2	8.20E-02
18°	501.8	427.4	74.62
30°	860.4	656.2	204.6
45°	1.30E+03	845.7	447.44
64°	1.71E+03	942.3	766.6
90°	2.30E+03	768.5	1.50E+03
117°	2.50E+03	187.5	2.30E+03
135°	2.40E+03	-203.4	2.60E+03
162°	1.20E+03	-1.04E+03	2.90E+03
180°	1.50E+03	-1.50E+03	2.96E+03

(a)

	R/X= 1		
δ	$P_{1,avg}$ (W)	$P_{2,avg}$ (W)	P_{R_line} (W)
0°	-4.25	-4.3	5.10E-02
18°	313	229.4	83.8
30°	598.6	342.2	256.5

45°	950.54	392.3	558
64°	1.30E+03	349.1	952.3
90°	1.90E+03	6.8	1.89E+03
117°	2.20E+03	-576.1	2.80E+03
135°	2.30E+03	-916	3.20E+03
162°	2.10E+03	-1.60E+03	3.60E+03
180°	1.90E+03	-1.85E+03	3.70E+03

(b)

	R/X= 3		
δ	$P_{1,avg}$ (W)	$P_{2,avg}$ (W)	P_{R_line} (W)
0°	-3.5	-3.6	1.02E-01
18°	84.6	28.1	56.5
30°	170.8	16.7	154.1
45°	3.03E+02	-33.6	336.2
64°	4.94E+02	-149	643.1
90°	7.64E+02	-375.8	1.10E+03
117°	9.98E+02	-647.2	1.60E+03
135°	1.10E+03	-822	1.90E+03
162°	1.20E+03	-1.00E+03	2.20E+03
180°	1.10E+03	-1.10E+03	2.30E+03

(c)
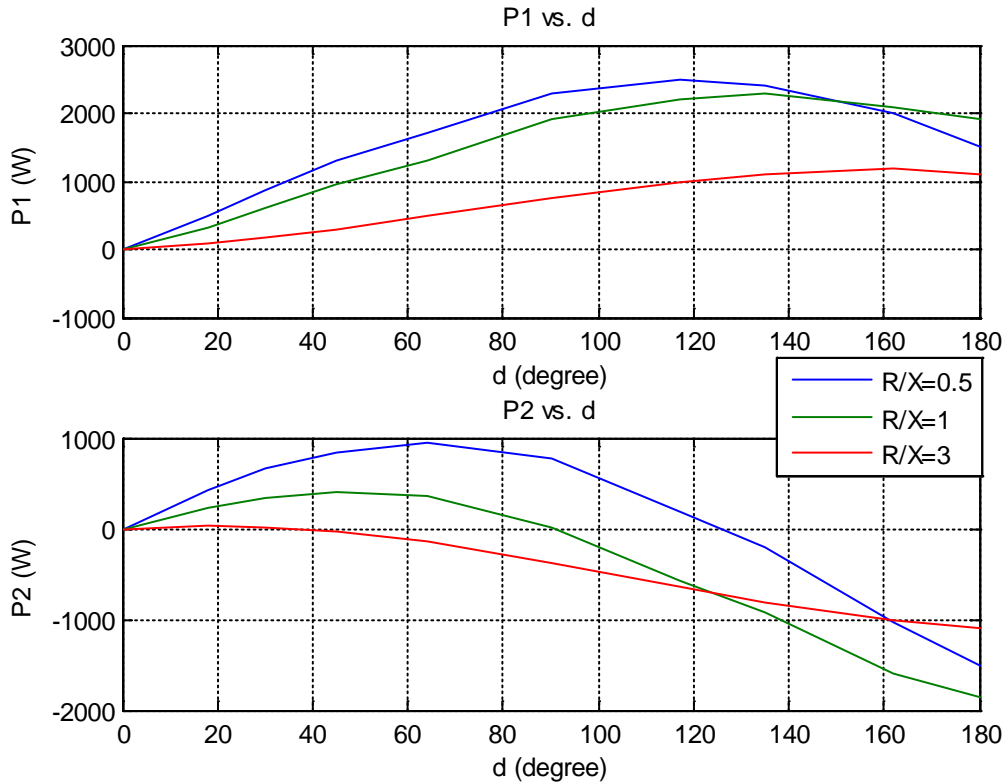
Fig. 4.3: The real power of the inverter and the real power of the grid at different R/X

ratios.

The figure shows δ increases for the power of the inverter and decreases for the grid power as R/X increases. Table 4.9 shows δ at which the power is maximized for the tested R/X ratios.

Table 4.9: The phase angles of maximum power

R/X	$\delta_{P1,max}$	$\delta_{P2,max}$
0.5	117°	64°
1	135°	45°
3	162°	18°

The power when R/X is not included above. SIMPLIS provides harmonic analysis of the plotted variables. And from the harmonic analysis, the harmonic contents of the

current and the harmonic contents of the grid voltage are found as shown in Table 4.10.

Table 4.10: A SIMPLIS sample of the harmonic components of the current and the grid voltage

Frequency	I(Spectrum(I_line))	V(Spectrum(Vgrid))
0	(17.02610505 ,0)	(-5.827e-006 ,0)
60	(-4.16411688 ,15.79852387)	(-6.812e-006 ,119.9995169)
120	(0.01284157 ,-0.0046038)	(5.637e-006 ,1.02e-005)
180	(0.00225181 ,0.018999569)	(0.000141015 ,4.3738e-005)
240	(-0.00489772 ,-0.00521505)	(6.2005e-006 ,-9.867e-006)
300	(0.010685572 ,-0.00833025)	(-0.00013986 ,-0.00015311)
360	(-0.0016104 ,0.004565188)	(-1.163e-005 ,-6.539e-007)

The power is calculated based on the harmonic contents of the current and the grid voltage at specific δ's.

Table 4.11: The current and the grid voltage calculated from the harmonic contents

δ	$\bar{I}$ (A)	$\bar{V}_{grid}$(V)	Power at the grid (W)
0°	0.058∟77.7°	120∟0°	1.5
30°	16.34∟-14.76°	120∟0°	1897.11
45°	24.163∟-22.3°	120∟0°	2688.69
60°	31.59∟-29.7°	120∟0°	3292.42
90°	44.69∟-44.8°	120∟0°	3804.05

The power when δ is 90° is 3804.05 W which is close to the power calculated from the equation. Therefore, the maximum power when R/X is 0 is at 90°.

Additionally, simulated power losses are shown in Fig. 4.4. Power loss at R/X of 0 is zero. But, power losses exist for other R/X ratios. The losses increase from R/X= 0 until R/X= 1. Then, the losses decrease as R/X goes higher because the line current decreases by increasing R/X ratio for values upper than 1. Also, the losses increase as the angle of the output voltage of the inverter increases.
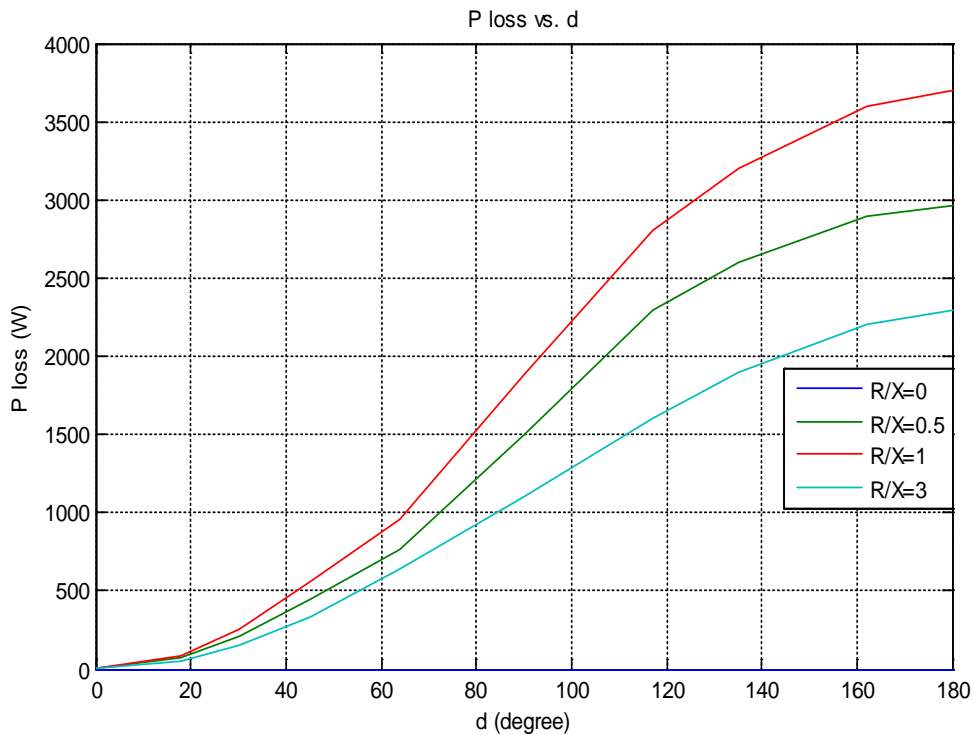
Fig. 4.4: Power losses for different R/X ratios.

4.4 Comparison between the Theoretical and Simulated Results

The results being compared are the angle of the maximum power for different R/X ratios, the power when R/X is 0 at specific quantities of δ, and the power loss in the line impedance. The maximum power angle at the selected R/X ratios are compared in Table 4.12.
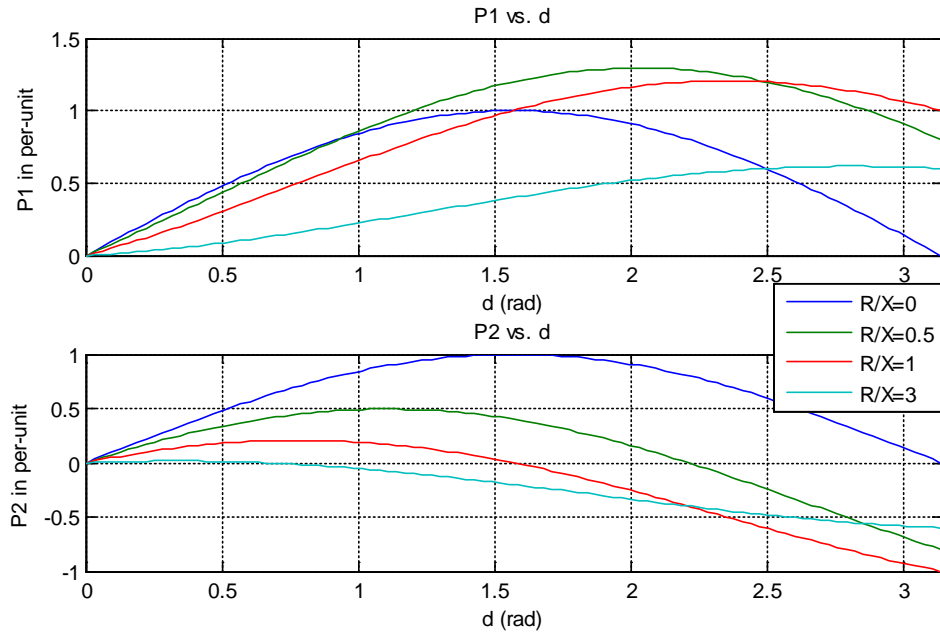
(a)
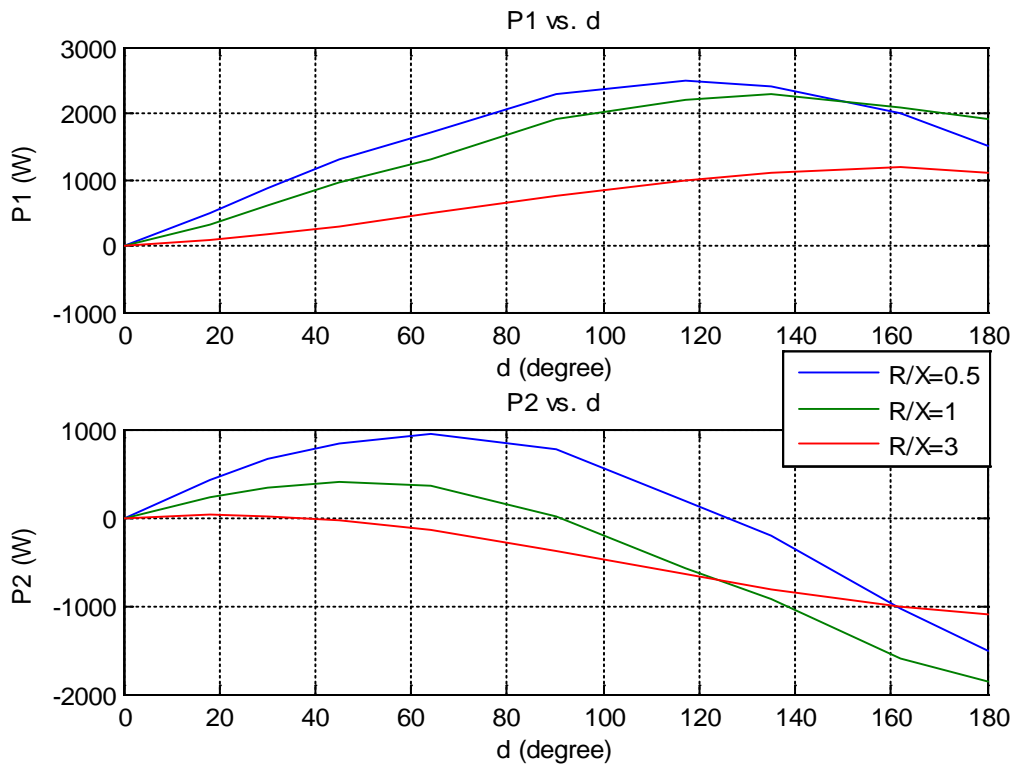
(b)

Fig. 4.5: (a) The theoretical real power versus δ. (b) The simulated real power versus δ.

Table 4.12: δ for maximum power of different R/X ratios

R/X	Theoretical δ		Simulated δ	
	$\delta_{P1,max}$	$\delta_{P2,max}$	$\delta_{P1,max}$	$\delta_{P2,max}$
0	90°	90°	90°	90°
0.5	116.36°	63.63°	≈117°	≈64°
1	134.54°	45.45°	≈135°	≈45°
3	161.82°	18.17°	≈162°	≈18°

From Fig. 4.5 and Table 4.12, δ for maximum power for a certain R/X ratio is approximately equal from both analyses. Moreover, the power at the grid when R/X equals to zero at different δ's is compared in the following table.

Table 4.13: Comparison of power when R/X equal to zero for different δ's

δ	$P_{2,Theoritical}$	$P_{2,Simulated}$	Error$_\%$
0°	0	1.5	NE
30°	1909.8	1897.11	0.66%
45°	2700.9	2688.69	0.45%
60°	3307.9	3292.42	0.46%
90°	3819.83	3804.05	0.41%

Notice that the error is very small and that the power calculated from both analyses are close to each other.

Finally, the power losses calculated from both analyses are compared to ensure that the both mathematical model and circuit model predict the same power loss.
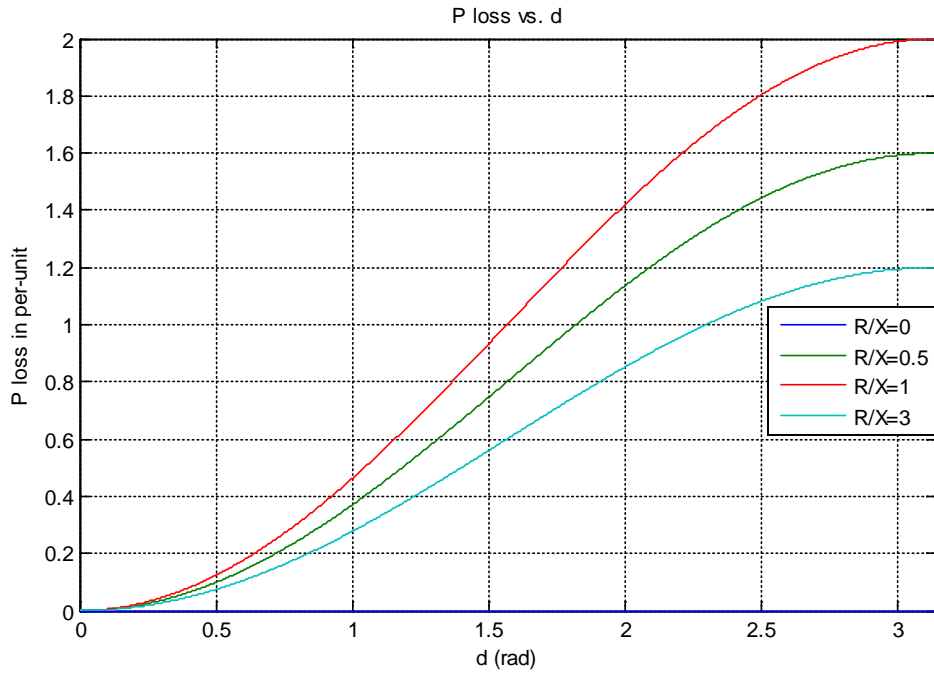
(a)
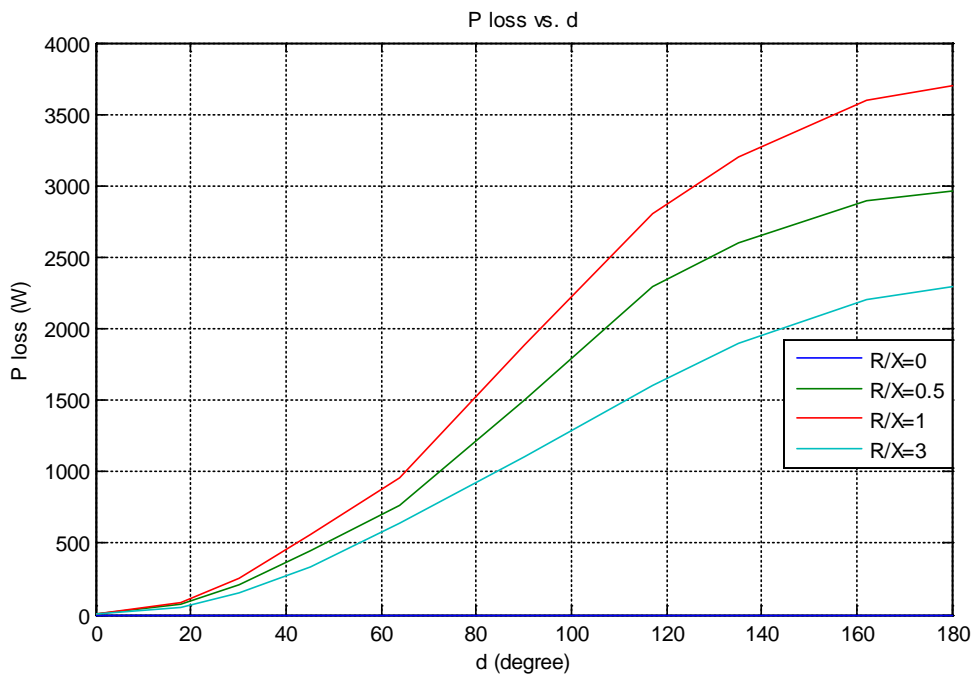
(b)

Fig. 4.6: (a) Power losses versus δ (Theoretical). (b) Power losses versus δ
(Simulated).

Fig. 4.6 shows that there are no power losses for R/X of zero in both graphs. Also, the

maximum losses occur when R/X equals to 1. The losses increase with increasing δ.

Both models have the same power losses. Thus, the curves of power losses are very similar.

5. Conclusion and Suggestions for Future Work

5.1 Suggestions for Future Work

For the future work, the SIMPLIS model that is built has ideal switches and diodes. These components must be replaced with practical switches and diodes. Tracking the maximum power point (MPPT) is one of the most important parts of a PV system in order to fully exploit the PV system [29]. By MPPT, the phase angle of the grid-tied inverter can be controlled [30] [31].   Also, another inverter topology could be used instead of the simple single phase central inverter proposed in this study. The multi-string inverter topology is becoming popular in recent applications because of high reliability, less power loss, and scalability of PV systems [24] [14]. Finally, since the variations of the grid impedance affect the system stability and performance. The inverters share the power perfectly when the line impedances are known. But, the grid impedance varies. Using the power sharing methods of the grid impedance estimation can help account for impedance variations [32-36]. These impedance estimation techniques ensure accurate active and reactive power sharing [32].

5.2 Conclusion

Interest in renewable energy systems continues to grow. The PV systems are one of the most popular types of the renewable energy systems. They are more likely to be found in grid connected systems. Many global utility companies are turning to PV systems to help meet peak power demand and reduce the need for building new power plants. A lot of issues have arisen from connecting PV systems to the utility grids.

In an attempt to help address some of the issues that the grid-connected PV systems suffer from, this research focused on the effects of the resistance of the distribution line on the maximum power transfer by building two models: a mathematical and a

simulation model. The resistance of the transmission line is usually ignored in the studies of high-voltage network. But, it is very important element to be included in the studies of distribution networks. Both models are studied and analyzed. The mathematical model was built to calculate the power of the grid, the power of the inverter, and the power losses, and then it was implemented in MATLAB to plot the results. Also, the performance of the system under variation of certain inputs and the power sensitivity to the variations of R and X were studied. The circuit model was simulated and measured in SIMPLIS and plotted in MATLAB. The mathematical model represented the theoretical study and the simulation model represented the experimental study. The results of both models can be summarized as:

- The power is sensitive to the grid impedance.

- The maximum power is affected by the resistance of the grid impedance.

- The amplitude of the power transferring to the grid decreases as R/X ratio increases.

- The phase angle (δ) for maximum power increases for the inverter power and decreases for the grid power as R/X ratio increases.

- The power of the grid and the power of the inverter when the R/X ratio is zero are equal; therefore, there are no power loss.

- The power losses increase as the R/X ratio increases from 0 to 1 and then it decreases as the R/X ratio increases.

- Power losses increase as δ increases.

References

[1]   Paul, J.S.; Sivan, A.P.; Balachandran, K., "Energy sector in India: Challenges and solutions," *Green Computing, Communication and Conservation of Energy (ICGCE), 2013 International Conference on* , pp.519,524, 12-14 Dec. 2013

[2]   Xia Xintao; Xia Junzi, "Evaluation of Potential for Developing Renewable Sources of Energy to Facilitate Development in Developing Countries," *Power and Energy Engineering Conference (APPEEC), 2010 Asia-Pacific* , pp.1,3, 28-31 March 2010

[3]   Omar Ellabban, Haitham Abu-Rub, Frede Blaabjerg, "Renewable energy resources: Current status, future prospects and their enabling technology," *Renewable and Sustainable Energy Reviews*, Volume 39, Pages 748-764, November 2014

[4]   Ghassemi, Abbas, *Introduction to Renewable Energy,*1st ed. Boca Raton, FL: Talyor & Francis Group, 2011, ch 1,6, pp 2-4, 99-100.

[5]   Lynn, Paul A., *Electricity from Sunlight An Introduction to Photovoltaics,* 1st ed. Chichester, UK: John Wiley & Sons, Ltd, 2010, ch 1,2,4, pp 1-25, 105-110.

[6]   Wolfe, P., "Advances in PV semiconductor materials and technology," *Developments in Photovoltaic Electricity Production (Digest No: 1997/069), IEE Colloquium on* , pp.1/1,1/4, 6 Mar 1997

[7]   Calais, M.; Myrzik, J.; Spooner, T.; Agelidis, V.G., "Inverters for single-phase grid connected photovoltaic systems-an overview," *Power Electronics Specialists Conference, 2002. pesc 02. 2002 IEEE 33rd Annual* , vol.4, pp.1995,2000, 2002

[8]   Venkatesan, M.; Rajeswari, R.; Keerthivasan, K., "A survey of single phase grid connected photovoltaic system," *Emerging Trends in Science, Engineering and Technology (INCOSET), 2012 International Conference on* , pp.404,408, 13-14 Dec. 2012

[9]   Shukla, M.; Sekar, A., "Study of the effect of X/R ratio of lines on voltage stability," *System Theory, 2003. Proceedings of the 35th Southeastern Symposium on* , pp.93,97, 16-18 March 2003

[10]   Yun Wei Li; Ching-Nan Kao, "An Accurate Power Control Strategy for Power-Electronics-Interfaced Distributed Generation Units Operating in a Low-Voltage Multibus Microgrid," *Power Electronics, IEEE Transactions on*, vol.24, no.12, pp.2977,2988, Dec. 2009

[11]   Blazic, B.; Papic, I., "Voltage profile support in distribution networks — influence of the network R/X ratio," *Power Electronics and Motion Control Conference, 2008. EPE-PEMC 2008. 13th* , pp.2510,2515, 1-3 Sept. 2008

[12]   Xiaofeng Sun; Yanjun Tian; Zhe Chen, "Adaptive decoupled power control method for inverter connected DG," *Renewable Power Generation, IET* , vol.8, no.2, pp.171,182, March 2014

[13]   Chien Liang Chen; Jih-Sheng Lai; Martin, D.; Yuang-Shung Lee, "State-space modeling, analysis, and implementation of paralleled inverters for microgrid applications," *Applied Power Electronics Conference and Exposition (APEC), 2010 Twenty-Fifth Annual IEEE* , pp.619,626, 21-25 Feb. 2010

[14]   Johnson, B., A., "Modeling and Analysis of A PV Grid-Tied Smart Inverter's Support Functions," M.S. thesis, EE. Dept., CSU, San Luis Obispo, CA, 2013.

[15] Yektay, N.; Darudi, A.; Javidi, M.H., "An optimal power flow control method for grid-connected inverters," *Environment and Electrical Engineering (EEEIC), 2013 13th International Conference on* , pp.260,265, 1-3 Nov. 2013

[16] Y. Chen and K. Smedley, "Three-Phase Boost-Type Grid-Connected Inverter," *IEEE Transactions on Power Electronics* , vol. 23, no. 5, pp. 2301–2309, Sep. 2008.

[17] Xiang Hao; Xu Yang; Tao Liu; Lang Huang; Wenjie Chen, "A Sliding-Mode Controller With Multiresonant Sliding Surface for Single-Phase Grid-Connected VSI With an LCL Filter," *Power Electronics, IEEE Transactions on* , vol.28, no.5, pp.2259,2268, May 2013

[18] Picardi, C.; Sgro, D., "Grid-connected inverter power flow control based on a new modeling approach of electrical signals," *Clean Electrical Power, 2009 International Conference on* , pp.585,590, 9-11 June 2009

[19] Lian Shu; Jinghong Zheng; Xinwei Shen; Huiyang Yin; Jinxia Li, "Parameters' sensitivity analysis of grid-connected photovoltaic power generation model under different kinds of disturbances," *Electrical & Electronics Engineering (EEESYM), 2012 IEEE Symposium on* , pp.658,661, 24-27 June 2012

[20] Zhanping Chen; Roy, K.; Tan-Li Chou, "Power sensitivity-a new method to estimate power dissipation considering uncertain specifications of primary inputs," *Computer-Aided Design, 1997. Digest of Technical Papers., 1997 IEEE/ACM International Conference on* , pp.40,44, 9-13 Nov. 1997

[21] SIMPLIS Technologies. [Online]. http://www.simplistechnologies.com/

[22] Bratt, J., "Grid Connected PV Inverter: modeling and simulation," M.S. thesis, EE. Dept., SDSU, San Diego, CA, 2011.

[23]   Jing Huang; Padmanabhan, K.; Collins, O.M., "The Sampling Theorem With Constant Amplitude Variable Width Pulses," *Circuits and Systems I: Regular Papers, IEEE Transactions on* , vol.58, no.6, pp.1178,1190, June 2011

[24]   Xiaoyan Li; Dairun Zhang; Yuan Li; Yang Xu, "Multi-String Photovoltaic Grid-Connected Inverter Based on Alternate Single-Phase PWM Control," *Power and Energy Engineering Conference (APPEEC), 2012 Asia-Pacific* , pp.1,4, 27-29 March 2012

[25]   Mohamed, Y.A.-R.I.; El-Saadany, E.F., "A Control Method of Grid-Connected PWM Voltage Source Inverters to Mitigate Fast Voltage Disturbances," *Power Systems, IEEE Transactions on* , vol.24, no.1, pp.489,491, Feb. 2009

[26]   Nelms, R., Power Electronics Lecture Notes, 2013.

[27]   Sun J., *Dynamics and Control of Switched ElectronicSystems,*London, UK: Springer,   Ltd,   2012,   ch   2,   pp   50.   [Online] http://www.springer.com/us/book/9781447128847

[28]   Hanju Cha; Trung-Kien Vu, "Comparative analysis of low-pass output filter for single-phase grid-connected Photovoltaic inverter," *Applied Power Electronics Conference and Exposition (APEC), 2010 Twenty-Fifth Annual IEEE* , pp.1659,1665, 21-25 Feb. 2010

[29]   Esram, T.; Chapman, P.L., "Comparison of Photovoltaic Array Maximum Power Point Tracking Techniques," *Energy Conversion, IEEE Transactions on* , vol.22, no.2, pp.439,449, June 2007

[30]   Wenhao Cai; Hui Ren; Yanjun Jiao; Mingwei Cai; Xiangpu Cheng, "Analysis and simulation for grid-connected photovoltaic system based on MATLAB," *Electrical and Control Engineering (ICECE), 2011 International Conference on* , pp.63,66, 16-18 Sept. 2011

[31] Quamruzzaman, M.; Rahman, K.M., "Development of a new phase-angle controlled grid-connected PV system," *Electrical and Computer Engineering (ICECE), 2010 International Conference on* , pp.82,85, 18-20 Dec. 2010

[32] Herong Gu; Xiaoqiang Guo; Weiyang Wu, "Accurate power sharing control for inverter-dominated autonomous microgrid," *Power Electronics and Motion Control Conference (IPEMC), 2012 7th International* , pp.368,372, 2-5 June 2012

[33] Carotenuto, P., L., "Grid impedance estimation in PV grid connectedsystems through PQ variation methods.A Simulink-based approach," M.S. thesis, EE. Dept., Universitat Politecnica de Catalunya, Barcelona, Espain, 2011

[34] Liserre, M.; Blaagjerg, F.; Teodorescu, R., "Grid impedance detection via excitation of LCL-filter resonance," *Industry Applications Conference, 2005. Fourtieth IAS Annual Meeting. Conference Record of the 2005* , pp.910,916 Vol. 2, 2-6 Oct. 2005

[35] Jing Yang; Tongwen Chen; Min Wu, "Online impedance matrix estimation of interconnected power systems," *Electrical Power & Energy Conference (EPEC), 2009 IEEE* , pp.1,5, 22-23 Oct. 2009

[36] Guoqiao Shen; Jun Zhang; Xiao Li; Chengrui Du; Dehong Xu, "Current control optimization for grid-tied inverters with grid impedance estimation," *Applied Power Electronics Conference and Exposition (APEC), 2010 Twenty-Fifth Annual IEEE* , pp.861,866, 21-25 Feb. 2010

APPENDIX A

A.1 MATLAB Code for Calculating the Maximum

```matlab
V1=1;      % Inverter voltage
V2=1;      % Grid voltage
d=linspace(0,pi);     % The phase angle of the inverter
voltage
X= 1;   %Assumed
R=[0 0.5 1 3];
for i=1:100
    for j=1:4
        P1(i,j)=                        (R(j)*V1^2-
R(j)*V1*V2*cos(d(i))+X*V1*V2*sin(d(i)))/(R(j)^2+X^2);
        P2(i,j)=                   (R(j)*V1*V2*cos(d(i))-
R(j)*V2^2+X*V1*V2*sin(d(i)))/(X^2+R(j)^2);
        P_lost(i,j)=P1(i,j)-P2(i,j);
end
end
figure(1)
subplot(2,1,1);
plot(d,P1)
xlabel('delta');
ylabel('P1 in per-unit');
title('P vs. d');
grid on;
subplot(2,1,2);
plot(d,P2)
xlabel('delta');
ylabel('P2 in per-unit');
title('P2 vs. d');
grid on;
figure(2)
plot(d,P_lost)
xlabel('delta');
ylabel('P lost in per-unit');
title('P lost vs. d');
grid on;
```

A.2 A SIMPLIS Sample of Voltage and Current Harmonic Data

	δ= 30°	
Frequency	V(Spectrum(Vgrid))	I(Spectrum(I_line))
0	(-5.827e-006 ,0)	(17.02610505 ,0)
10	(-3.957e-005 ,-6.684e-005)	(-17.0299928 ,-0.03873553)
20	(9.0789e-005 ,0.000133682)	(0.003094757 ,0.008275408)
30	(-4.254e-005 ,-6.65e-005)	(0.000446517 ,0.00222521)
40	(-5.707e-006 ,-6.779e-007)	(-8.173e-005 ,0.00107013)
50	(6.2596e-006 ,-59.9997581)	(2.082864187 ,-7.8997116)
60	(-6.812e-006 ,119.9995169)	(-4.16411688 ,15.79852387)
70	(1.7373e-006 ,-59.9997608)	(2.081573041 ,-7.89781329)
80	(3.3372e-006 ,4.6587e-006)	(6.0406e-005 ,-0.0001631)
90	(5.47e-005 ,-0.00012001)	(1.9493e-005 ,7.198e-005)
100	(-0.00011274 ,0.000235362)	(8.2593e-005 ,9.2364e-005)
110	(5.3551e-005 ,-0.00012278)	(-0.00670721 ,0.001837322)
120	(5.637e-006 ,1.02e-005)	(0.01284157 ,-0.0046038)
130	(7.2422e-005 ,-6.98e-006)	(-0.00603667 ,0.002807966)
140	(-0.00015048 ,3.76e-006)	(-8.279e-005 ,-7.117e-005)
150	(7.4158e-005 ,-4.551e-006)	(-1.03e-005 ,-5.184e-006)
160	(2.1657e-006 ,5.3419e-006)	(7.4264e-005 ,2.3018e-005)
170	(-7.159e-005 ,-2.454e-005)	(-0.00150586 ,-0.00949363)
180	(0.000141015 ,4.3738e-005)	(0.00225181 ,0.018999569)
190	(-7.174e-005 ,-1.929e-005)	(-0.00075783 ,-0.00957066)
200	(2.4632e-006 ,-5.155e-006)	(-7.374e-005 ,3.6099e-005)
210	(-3.02e-005 ,5.2301e-005)	(-2.783e-005 ,3.2907e-006)
220	(5.7947e-005 ,-9.945e-005)	(5.9195e-005 ,-4.391e-005)
230	(-3.207e-005 ,5.4657e-005)	(0.002312479 ,0.002842814)
240	(6.2005e-006 ,-9.867e-006)	(-0.00489772 ,-0.00521505)
250	(-3.808e-005 ,-2.634e-005)	(0.002512413 ,0.002358277)
260	(6.9957e-005 ,6.255e-005)	(-4.289e-006 ,7.2018e-005)
270	(-3.68e-005 ,-2.903e-005)	(-7.863e-006 ,1.6149e-006)
280	(3.6448e-006 ,-4.487e-006)	(-1.669e-005 ,-3.09e-005)
290	(6.8106e-005 ,7.8796e-005)	(-0.00524071 ,0.004313986)
300	(-0.00013986 ,-0.00015311)	(0.010685572 ,-0.00833025)
310	(7.2771e-005 ,7.6389e-005)	(-0.00547518 ,0.004051229)
320	(-5.686e-006 ,3.2831e-007)	(3.1247e-005 ,2.2814e-005)
330	(-2.227e-005 ,-4.089e-005)	(8.3584e-006 ,1.621e-005)
340	(5.0235e-005 ,8.1461e-005)	(-3.774e-005 ,-1.55e-005)
350	(-1.93e-005 ,-4.04e-005)	(0.000931319 ,-0.00229229)
360	(-1.163e-005 ,-6.539e-007)	(-0.0016104 ,0.004565188)
370	(-6.148e-006 ,2.9483e-005)	(0.000697993 ,-0.00223079)
380	(2.3929e-005 ,-5.831e-005)	(1.5366e-005 ,-1.788e-005)
390	(-9.112e-006 ,2.9672e-005)	(8.4438e-006 ,4.638e-006)
400	(-5.704e-006 ,-1.031e-006)	(-6.788e-006 ,1.4994e-005)